

\mathcal{H}_2 -OPTIMAL MODEL REDUCTION USING PROJECTED NONLINEAR LEAST SQUARES*

JEFFREY M. HOKANSON[†] AND CALEB C. MAGRUDER[‡]

Abstract. In many applications throughout science and engineering, model reduction plays an important role replacing expensive large-scale linear dynamical systems by inexpensive reduced order models that capture key features of the original, full order model. One approach to model reduction finds reduced order models that are locally optimal approximations in the \mathcal{H}_2 norm, an approach taken by the Iterative Rational Krylov Algorithm (IRKA) among others. Here we introduce a new approach for \mathcal{H}_2 -optimal model reduction using the projected nonlinear least squares framework previously introduced in [J. M. Hokanson, SIAM J. Sci. Comput. 39 (2017), pp. A3107–A3128]. At each iteration, we project the \mathcal{H}_2 optimization problem onto a finite-dimensional subspace yielding a weighted least squares rational approximation problem. Subsequent iterations append this subspace such that the least squares rational approximant asymptotically satisfies the first order necessary conditions of the original, \mathcal{H}_2 optimization problem. This enables us to build reduced order models with similar error in the \mathcal{H}_2 norm but using far fewer evaluations of the expensive, full order model compared to competing methods. Moreover, our new algorithm only requires access to the transfer function of the full order model, unlike IRKA which requires a state-space representation or TF-IRKA which requires both the transfer function and its derivative. Applying the projected nonlinear least squares framework to the \mathcal{H}_2 -optimal model reduction problem open new avenues for related model reduction problems.

Key words. model reduction, \mathcal{H}_2 approximation, projected nonlinear least squares, rational approximation, transfer function

AMS subject classifications. 41A20, 46E22, 90C53, 93A15, 93C05, 93C15

DOI.

1. Introduction. Model reduction seeks to replace an expensive, high-fidelity model of a system with a low-dimensional, inexpensive surrogate. Although the cost of building this *reduced order model* (ROM) is oftentimes on the order of evaluating the original *full order model* (FOM), this cost is justified in two settings: many-query settings, such as optimization and uncertainty quantification, and in real-time applications where the cost of the full order simulation is unaffordable online. There are a wide variety of techniques for model reduction, such as Balanced Truncation, Proper Orthogonal Decomposition (POD), and interpolatory methods; for an extensive overview, see [11]. In this paper, we address the \mathcal{H}_2 -optimal model reduction problem—a model reduction approach requiring both the full and reduced order models to be described by a stable, linear, time-invariant dynamical system. In this setting, the action of these models are completely defined through either their *impulse response* h or their *transfer function* H , the Laplace transform of h . Under these assumptions, the transfer function H is an element of the \mathcal{H}_2 Hilbert space: the space of functions analytic in the closed right half plane along with the inner product

$$(1.1) \quad \langle F, G \rangle_{\mathcal{H}_2} := \frac{1}{2\pi} \int_{-\infty}^{\infty} \overline{F(i\omega)} G(i\omega) d\omega, \quad F, G \in \mathcal{H}_2, \quad i := \sqrt{-1}.$$

*Submitted to the editors 15 June 2018.

Funding: The first author’s work is partially supported by DARPA’s program Enabling Quantification of Uncertainty in Physical Systems (EQUIPS).

[†] Department of Computer Science, University of Colorado Boulder, 1111 Engineering Dr, Boulder, CO 80309, (Jeffrey.Hokanson@colorado.edu).

[‡] The MathWorks Inc., 1 Apple Hill Drive, Natick, MA, 01760-2098 (ccmagruder@gmail.com)

Given a space of candidate reduced order models whose transfer functions are in the set $\mathcal{M} \subset \mathcal{H}_2$, the goal of \mathcal{H}_2 -optimal model reduction is to find the element $H_r \in \mathcal{M}$ that is closest to the transfer function of the full order model H in the \mathcal{H}_2 -norm

$$(1.2) \quad \min_{H_r \in \mathcal{M}} \|H - H_r\|_{\mathcal{H}_2}^2 \quad \text{where} \quad \|F\|_{\mathcal{H}_2}^2 := \langle F, F \rangle_{\mathcal{H}_2}.$$

As we consider a case where \mathcal{M} is nonconvex, we consider local optimizers satisfying the first order optimality conditions as solutions to (1.2).

Here we introduce a new approach for solving the \mathcal{H}_2 -optimal model reduction problem based on the projected nonlinear least squares framework introduced in [30]. The core of this approach consists of approximating a Hilbert space norm by introducing a sequence of orthogonal projectors. For the model reduction problem, we introduce the orthogonal projector $P(\boldsymbol{\mu})$ into (1.2) and solve the *projected problem*

$$(1.3) \quad \min_{H_r \in \mathcal{M}} \|P(\boldsymbol{\mu})[H - H_r]\|_{\mathcal{H}_2}^2.$$

We construct this projector $P(\boldsymbol{\mu})$ so that projected norm can be evaluated as a weighted ℓ_2 norm of $H - H_r$ evaluated at *interpolation points* $\boldsymbol{\mu} = [\mu_1, \dots, \mu_n]$,

$$(1.4) \quad \|P(\boldsymbol{\mu})(H - H_r)\|_{\mathcal{H}_2}^2 = \left\| \mathbf{M}(\boldsymbol{\mu})^{-\frac{1}{2}} \left(\begin{bmatrix} H(\mu_1) \\ \vdots \\ H(\mu_n) \end{bmatrix} - \begin{bmatrix} H_r(\mu_1) \\ \vdots \\ H_r(\mu_n) \end{bmatrix} \right) \right\|_2^2$$

where $\mathbf{M}(\boldsymbol{\mu})$, defined in (4.7), acts to preserve the norm. This equivalence is possible due to the reproducing kernel Hilbert space structure of \mathcal{H}_2 (see subsection 2.2). By introducing the projector, we are able to solve the projected problem (1.3) using standard nonlinear least squares techniques provided a parameterization of \mathcal{M} ; we refer to this as *inner loop*.

Around this inner loop we construct an *outer loop* updating the projector $P(\boldsymbol{\mu})$ such that local optimizers of the projected problem (1.3) converge to a local optimizer of the original problem (1.2). The following lemma provides the key insight connecting local optimizers of these two problems.

LEMMA 1.1. *Suppose \mathcal{M} admits a parameterization $H_r(\cdot; \boldsymbol{\theta})$ where $\boldsymbol{\theta} \in \mathcal{D} \subset \mathbb{R}^p$ and \mathcal{D} is open. Let $\mathcal{T}(\boldsymbol{\theta})$ denote subspace containing the derivatives of H_r with respect to this parameterization,*

$$(1.5) \quad \mathcal{T}(\boldsymbol{\theta}) := \text{Span} \left\{ \left. \frac{\partial H_r(\cdot; \boldsymbol{\theta})}{\partial \theta_1} \right|_{\boldsymbol{\theta}=\boldsymbol{\theta}}, \dots, \left. \frac{\partial H_r(\cdot; \boldsymbol{\theta})}{\partial \theta_p} \right|_{\boldsymbol{\theta}=\boldsymbol{\theta}} \right\}.$$

If $H_r(\cdot; \hat{\boldsymbol{\theta}})$ is a local optimizer of the projected problem (1.3) and $\text{Range } P(\boldsymbol{\mu}) \supseteq \mathcal{T}(\hat{\boldsymbol{\theta}})$, then $H_r(\cdot; \hat{\boldsymbol{\theta}})$ is also a local optimizer of the original problem (1.2).

Proof. If $H_r(\cdot; \hat{\boldsymbol{\theta}}) \in \mathcal{M}$ is a local optimizer of either the original (1.2) or projected (1.3) problems, then

$$(1.6) \quad \langle H - H_r(\cdot; \hat{\boldsymbol{\theta}}), T \rangle_{\mathcal{H}_2} = 0 \quad \forall T \in \mathcal{T}(\hat{\boldsymbol{\theta}}) \quad (\text{original}),$$

$$(1.7) \quad \langle P(\boldsymbol{\mu})[H - H_r(\cdot; \hat{\boldsymbol{\theta}})], T \rangle_{\mathcal{H}_2} = 0 \quad \forall T \in \mathcal{T}(\hat{\boldsymbol{\theta}}) \quad (\text{projected}).$$

As $P(\boldsymbol{\mu})$ is an orthogonal projector we can move it into the right argument of (1.7). Then for all $T \in \mathcal{T}(\hat{\boldsymbol{\theta}})$, we note $P(\boldsymbol{\mu})T = T$ as $\text{Range } P(\boldsymbol{\mu}) \supseteq \mathcal{T}(\hat{\boldsymbol{\theta}})$ and consequently

$$(1.8) \quad \langle P(\boldsymbol{\mu})[H - H_r(\cdot; \hat{\boldsymbol{\theta}})], T \rangle_{\mathcal{H}_2} = \langle H - H_r(\cdot; \hat{\boldsymbol{\theta}}), P(\boldsymbol{\mu})T \rangle_{\mathcal{H}_2} = \langle H - H_r(\cdot; \hat{\boldsymbol{\theta}}), T \rangle_{\mathcal{H}_2}.$$

Hence if $H_r(\cdot; \hat{\boldsymbol{\theta}})$ satisfies (1.7), then $H_r(\cdot; \hat{\boldsymbol{\theta}})$ satisfies (1.6). \square

Motivated by this insight, we design the outer loop to increase the range of the projector $P(\boldsymbol{\mu})$ such that (asymptotically) we satisfy the containment requirement of Lemma 1.1. To maximize reuse existing evaluations of the transfer function, each iteration of the outer loop adds an interpolation point to the projector; i.e.,

$$(1.9) \quad \boldsymbol{\mu}^+ = [\mu_1, \dots, \mu_n, \mu_{n+1}] \implies \text{Range } P(\boldsymbol{\mu}) \subset \text{Range } P(\boldsymbol{\mu}^+).$$

1.1. Space of ROMs. Although the projected nonlinear least squares framework can be applied to any family of reduced order models \mathcal{M} with a finite-dimensional parameterization, the details of both the inner and outer loop depend on this choice. Due to their popularity, here we restrict our attention to state-space reduced order models posed over the field \mathbb{F} that is either real \mathbb{R} or complex \mathbb{C}

$$(1.10) \quad \left\{ \begin{array}{l} \mathbf{x}'_r(t) = \mathbf{A}_r \mathbf{x}_r(t) + \mathbf{b}_r u(t), \quad \mathbf{x}_r(0) = \mathbf{0} \\ y_r(t) = \mathbf{c}_r^* \mathbf{x}_r(t) \end{array} \right\} \quad \text{where } \mathbf{A}_r \in \mathbb{F}^{r \times r}, \mathbf{b}_r, \mathbf{c}_r \in \mathbb{F}^r$$

and whose transfer function is

$$(1.11) \quad H_r(z; \mathbf{A}_r, \mathbf{b}_r, \mathbf{c}_r) := \mathbf{c}_r^* [z\mathbf{I} - \mathbf{A}_r]^{-1} \mathbf{b}_r.$$

This transfer function is a degree $(r-1, r)$ rational function as the resolvent $[z\mathbf{I} - \mathbf{A}_r]^{-1}$ is a degree $(r-1, r)$ matrix-valued rational function [33, Chap. 1, eq. (5.23)]. We denote the space of $(r-1, r)$ scalar-valued rational functions as

$$(1.12) \quad \mathcal{R}_r(\mathbb{F}) := \left\{ \frac{p}{q} : p \in \mathcal{P}_{r-1}(\mathbb{F}), q \in \mathcal{P}_r(\mathbb{F}) \right\}$$

where $\mathcal{P}_r(\mathbb{F})$ denotes polynomials of degree r with coefficients in the field \mathbb{F} . There is a surjective mapping between state-space transfer functions (1.11) and elements of $\mathcal{R}_r(\mathbb{F})$; hence for any rational function $H_r \in \mathcal{R}_r(\mathbb{F})$ we can nonuniquely identify a state-space system with matrices $\mathbf{A} \in \mathbb{F}^{r \times r}$, and $\mathbf{b}, \mathbf{c} \in \mathbb{F}^r$ whose transfer function is H_r . Not all elements of $\mathcal{R}_r(\mathbb{F})$ are members of \mathcal{H}_2 . For $H_r \in \mathcal{R}_r(\mathbb{F})$ to be in \mathcal{H}_2 all its poles must lie in the open left half plane. We denote this space as

$$(1.13) \quad \mathcal{R}_r^+(\mathbb{F}) := \left\{ \frac{p}{q} : p \in \mathcal{P}_{r-1}(\mathbb{F}), q \in \mathcal{P}_r(\mathbb{F}), \forall q(\lambda) = 0 \implies \text{Re } \lambda < 0 \right\} = \mathcal{R}_r(\mathbb{F}) \cap \mathcal{H}_2.$$

As many applications of model reduction in science and engineering involve real dynamical systems—e.g., diffuse optimal tomography [19, 38], structural mechanics [25, 42], thermal dynamics [16], and optimal control [25]—here we focus our attention to finding real reduced order models $H_r \in \mathcal{R}_r^+(\mathbb{R})$.

1.2. Advantages. There are two main advantages to our *Projected* \mathcal{H}_2 approach compared to existing methods for \mathcal{H}_2 -optimal model reduction.

One advantage of our Projected \mathcal{H}_2 approach is that it only requires evaluations of the full order model transfer function $H(\mu_j)$. This places minimal requirements on the full order model. In contrast, the Iterative Rational Krylov Algorithm (IRKA) [28] requires state-space representation of the full order model. Other methods require evaluating derivatives of the transfer function; e.g., Transfer Function IRKA (TF-IRKA) [6] requires first derivatives and Newton methods [10, 36] require both first and second derivatives. Quadrature-based Vector Fitting (QuadVF) [23] does not require derivatives, but does need a particular limit of H .

Another benefit is practical: our method typically yields comparable or better reduced order models using fewer evaluations of the full order model. This is significant because for large scale models, evaluating $H(z)$ dominates the cost; e.g., if $H(z)$ is the transfer function of a large state-space system

$$(1.14) \quad \left\{ \begin{array}{l} \mathbf{x}'(t) = \mathbf{A}\mathbf{x}(t) + \mathbf{b}u(t), \quad \mathbf{x}(0) = \mathbf{0} \\ y(t) = \mathbf{c}^*\mathbf{x}(t) \end{array} \right\} \quad \text{where} \quad \begin{array}{l} \mathbf{A} \in \mathbb{C}^{n \times n}, \quad \mathbf{b}, \mathbf{c} \in \mathbb{C}^n \\ H(z) = \mathbf{c}^*[z\mathbf{I} - \mathbf{A}]^{-1}\mathbf{b}, \end{array}$$

then the cost of evaluating $H(z)$ is dominated by the linear solve. As the numerical experiments in section 7 demonstrate, our Projected \mathcal{H}_2 approach uses fewer transfer function evaluations than both IRKA and TF-IRKA—often by an order of magnitude. This is because each iteration of Projected \mathcal{H}_2 recycles previous evaluations of $H(\mu_j)$, whereas each iteration of standard IRKA and TF-IRKA discards these evaluations and requires $2r$ evaluations. Similarly, our algorithm tends to find better local minimizers because each inner loop of Projected \mathcal{H}_2 solves an overdetermined rational approximation problem where we are able to try multiple initializations. In contrast, the rational interpolant generated by IRKA and TF-IRKA at each step is unique. Both Projected \mathcal{H}_2 and QuadVF are similar in that they solve overdetermined rational approximation problems, however they differ in how the \mathcal{H}_2 norm is approximated. QuadVF uses a fixed quadrature rule evaluating H on the imaginary axis whereas our approach projects the \mathcal{H}_2 norm as in (1.3) evaluating H in the right half plane. By dynamically projecting the \mathcal{H}_2 norm, our approach tends to better approximate the \mathcal{H}_2 -norm yielding better reduced order models.

2. Properties of the \mathcal{H}_2 Hilbert Space. To begin, we briefly summarize the properties of the \mathcal{H}_2 Hilbert space essential for the development of our algorithm.

2.1. Evaluation of \mathcal{H}_2 Norm. Although the \mathcal{H}_2 norm is defined through an integral in (1.1), when H has a state-space representation (1.14) we can compute this norm exactly. In this case the impulse response $h(t)$ and transfer function $H(z)$ are

$$(2.1) \quad h(t) = \mathbf{c}^* \exp[\mathbf{A}t]\mathbf{b} \quad \text{and} \quad H(z) = \mathbf{c}^*[z\mathbf{I} - \mathbf{A}]^{-1}\mathbf{b}.$$

Then the \mathcal{H}_2 norm can be computed from either the controllability \mathbf{W}_c or observability \mathbf{W}_o Gramians. Both Gramians are the solution to a Lyapunov equation [3, Sec. 4.3]:

$$(2.2) \quad \mathbf{W}_c := \int_0^\infty e^{\mathbf{A}t}\mathbf{b}\mathbf{b}^*e^{\mathbf{A}^*t} dt, \quad \mathbf{A}\mathbf{W}_c + \mathbf{W}_c\mathbf{A}^* = -\mathbf{b}\mathbf{b}^*;$$

$$(2.3) \quad \mathbf{W}_o := \int_0^\infty e^{\mathbf{A}^*t}\mathbf{c}\mathbf{c}^*e^{\mathbf{A}t} dt, \quad \mathbf{A}^*\mathbf{W}_o + \mathbf{W}_o\mathbf{A} = -\mathbf{c}\mathbf{c}^*.$$

Using either Gramian, the \mathcal{H}_2 -norm can be evaluated as [3, eq. (5.28)]

$$(2.4) \quad \|H\|_{\mathcal{H}_2}^2 := \frac{1}{2\pi} \int_{-\infty}^\infty |H(i\omega)|^2 d\omega = \int_0^\infty |h(t)|^2 dt = \mathbf{c}^*\mathbf{W}_c\mathbf{c} = \mathbf{b}^*\mathbf{W}_o\mathbf{b}.$$

2.2. Reproducing Kernel Hilbert Space. *Reproducing kernel Hilbert spaces* [4] are Hilbert spaces which contain a kernel $K[\mu]$ that is also the sampling operator, i.e., $\langle K[\mu], F \rangle = F(\mu)$. For the \mathcal{H}_2 Hilbert space this kernel is $v[\mu]$

$$(2.5) \quad v[\mu](z) := (z + \bar{\mu})^{-1} \quad \text{where} \quad \mu \in \mathbb{C}_+ := \{\mu \in \mathbb{C} : \text{Re } \mu > 0\}.$$

The reproducing property follows from the Cauchy integral formula [28, Lem. 2.4]

$$(2.6) \quad \begin{aligned} \langle v[\mu], H \rangle_{\mathcal{H}_2} &= \frac{1}{2\pi} \int_{-\infty}^{\infty} \overline{v[\mu](i\omega)} H(i\omega) d\omega = \frac{1}{2\pi} \int_{-\infty}^{\infty} \frac{1}{-i\omega + \mu} H(i\omega) d\omega \\ &= \frac{-1}{2\pi} \int_{-\infty}^{\infty} \frac{1}{i\omega - \mu} H(i\omega) d\omega = \frac{-i}{2\pi} \lim_{R \rightarrow \infty} \int_{D_R} \frac{1}{z - \mu} H(z) dz = H(\mu), \end{aligned}$$

where D_R denotes the counterclockwise path along the boundary of the right half disk of radius R split along the imaginary axis.

2.3. Meier-Luenberger Optimality Conditions. The first order optimality conditions for \mathcal{H}_2 model reduction by state-space systems are called the *Meier-Luenberger* conditions [35]. These follow from the optimality conditions (1.6), but are frequently presented as Hermite interpolation conditions through use of the reproducing kernel $v[\mu]$. Here we provide a brief derivation under the assumption $H_r \in \mathcal{R}_r^+(\mathbb{C})$ has only simple poles; for a derivation with out this constraint, see [22]. This assumption allows us to parameterize H_r in terms of poles $\lambda \in \mathbb{C}^r$ and residues $\rho \in \mathbb{C}^r$

$$(2.7) \quad H_r(z; \lambda, \rho) := \sum_{k=1}^r \frac{\rho_k}{z - \lambda_k} = \sum_{k=1}^r \rho_k v[-\overline{\lambda_k}](z), \quad \lambda, \rho \in \mathbb{C}^r, \lambda_k < 0.$$

Taking derivatives with respect to the real and imaginary parts yields:

$$(2.8) \quad \frac{\partial}{\partial \operatorname{Re} \lambda_k} \|H - H_r(\cdot; \lambda, \rho)\|_{\mathcal{H}_2}^2 = 2 \operatorname{Re} \langle \rho_k v[-\overline{\lambda_k}]', H - H_r(\cdot; \lambda, \rho) \rangle_{\mathcal{H}_2};$$

$$(2.9) \quad \frac{\partial}{\partial \operatorname{Im} \lambda_k} \|H - H_r(\cdot; \lambda, \rho)\|_{\mathcal{H}_2}^2 = -2 \operatorname{Re} \langle i \rho_k v[-\overline{\lambda_k}]', H - H_r(\cdot; \lambda, \rho) \rangle_{\mathcal{H}_2};$$

$$(2.10) \quad \frac{\partial}{\partial \operatorname{Re} \rho_k} \|H - H_r(\cdot; \lambda, \rho)\|_{\mathcal{H}_2}^2 = -2 \operatorname{Re} \langle v[-\overline{\lambda_k}], H - H_r(\cdot; \lambda, \rho) \rangle_{\mathcal{H}_2};$$

$$(2.11) \quad \frac{\partial}{\partial \operatorname{Im} \rho_k} \|H - H_r(\cdot; \lambda, \rho)\|_{\mathcal{H}_2}^2 = -2 \operatorname{Re} \langle i v[-\overline{\lambda_k}], H - H_r(\cdot; \lambda, \rho) \rangle_{\mathcal{H}_2};$$

where $v[\mu]'$ denotes the derivative of $v[\mu]$, $v[\mu]'(z) := -(z + \overline{\mu})^{-2}$. When the equations above are all zero, \widehat{H}_r satisfies the first order necessary conditions. Denoting these parameter values as $\widehat{\lambda}$ and $\widehat{\rho}$, combining terms pairwise and invoking (2.5) yields

$$(2.12) \quad 0 = \left\langle v[-\overline{\widehat{\lambda}_k}]', H - H_r(\cdot; \widehat{\lambda}, \widehat{\rho}) \right\rangle_{\mathcal{H}_2} \Leftrightarrow H'(-\overline{\widehat{\lambda}_k}) = H_r'(-\overline{\widehat{\lambda}_k}; \widehat{\lambda}, \widehat{\rho}),$$

$$(2.13) \quad 0 = \left\langle v[-\overline{\widehat{\lambda}_k}], H - H_r(\cdot; \widehat{\lambda}, \widehat{\rho}) \right\rangle_{\mathcal{H}_2} \Leftrightarrow H(-\overline{\widehat{\lambda}_k}) = H_r(-\overline{\widehat{\lambda}_k}; \widehat{\lambda}, \widehat{\rho}),$$

provided $|\widehat{\rho}_k| > 0$. These conditions require a locally optimal H_r to be a Hermite interpolant of H at the reflection of the poles $\widehat{\lambda}$ across the imaginary axis. This result applies to real reduced order models as well, since $\mathcal{R}_r^+(\mathbb{R})$ is a subspace of $\mathcal{R}_r^+(\mathbb{C})$

$$(2.14) \quad \mathcal{R}_r^+(\mathbb{R}) = \{F \in \mathcal{R}_r^+(\mathbb{C}) : \overline{F(z)} = F(\overline{z}) \forall z \in \mathbb{C}\}.$$

Further, although this parameterization explicitly excludes higher order poles—i.e., $H_r(z) = (z - \lambda)^{-2}$ cannot be expressed in this parameterization—in practice this is not a concern. Rational functions with higher order poles are nowhere dense in $\mathcal{R}_r^+(\mathbb{C})$ [22, p. 2739] and hence cannot be resolved in finite precision arithmetic.

Algorithm 3.1 Iterative Rational Krylov Algorithm (IRKA) (simplified)

Input : FOM system $\{\mathbf{A}, \mathbf{b}, \mathbf{c}\}$, initial interpolation points $\boldsymbol{\mu}^{(0)} = [\mu_1^{(0)}, \dots, \mu_r^{(0)}]$
Output : ROM system $\{\mathbf{A}_r, \mathbf{b}_r, \mathbf{c}_r\}$

- 1 **for** $\ell = 0, 1, 2, \dots$ **do**
- 2 Construct rational Krylov spaces \mathbf{V} and \mathbf{W} given $\boldsymbol{\mu}^{(\ell)}$ using (3.1) and (3.2);
- 3 Build state-space reduced order model $\{\mathbf{A}_r, \mathbf{b}_r, \mathbf{c}_r\}$ with \mathbf{V} and \mathbf{W} via (3.3);
- 4 Choose $\mu_j^{(\ell+1)} = -|\operatorname{Re} \lambda_j| - i \operatorname{Im} \lambda_j$ where $\{\lambda_j\}_{j=1}^r$ are eigenvalues of \mathbf{A}_r ;

3. Existing Algorithms. There are a variety of techniques for \mathcal{H}_2 -optimal model reduction. Each of these requires access to different information about the full order model described by H . For example, both IRKA [28] and TF-IRKA [6] are fixed point iterations based on rational interpolants, but IRKA requires access to a state-space representation of H whereas TF-IRKA only requires access to $H(z)$ and $H'(z)$. Van Dooren, Gallivan, and Absil propose a similar fixed point iteration that allows for higher order poles in the reduced order model [21, 22]. There are also Newton methods that require access to $H(z)$, $H'(z)$, and $H''(z)$, such as the approach developed by Meier [36] and a trust-region approach due to Beattie and Gugercin [10]. In addition to these optimal methods, there are also several suboptimal methods that require only access to $H(z)$. For example, QuadVF uses a quadrature rule to approximate the \mathcal{H}_2 -norm [23] and \mathcal{H}_2 pseudo-optimality removes the derivative condition from the Meier-Luenberger conditions and finds a reduced order model with fixed poles that minimizes the \mathcal{H}_2 norm [43]. In this section we briefly summarize three of these algorithms used as comparisons in section 7: IRKA, TF-IRKA, and QuadVF.

3.1. IRKA. The Iterative Rational Krylov Algorithm (IRKA) [28] builds on earlier work constructing rational interpolants for full order models given in state-space form [27, 44]. Given a state-space system (1.14) with matrices \mathbf{A} , \mathbf{b} , and \mathbf{c} , a Hermite rational interpolant at points $\{\mu_j\}_{j=1}^r$ can be constructed using rational Krylov spaces \mathcal{W} and \mathcal{V}

$$(3.1) \quad \mathcal{V} = \operatorname{Range}(\mathbf{V}) = \operatorname{Span}\{[\mu_1 \mathbf{I} - \mathbf{A}]^{-1} \mathbf{b}, \dots, [\mu_r \mathbf{I} - \mathbf{A}]^{-1} \mathbf{b}\}, \quad \mathbf{V}^* \mathbf{V} = \mathbf{I};$$

$$(3.2) \quad \mathcal{W} = \operatorname{Range}(\mathbf{W}) = \operatorname{Span}\{[\mu_1 \mathbf{I} - \mathbf{A}]^{-*} \mathbf{c}, \dots, [\mu_r \mathbf{I} - \mathbf{A}]^{-*} \mathbf{c}\}, \quad \mathbf{W}^* \mathbf{W} = \mathbf{I}.$$

Then the reduced order model $H_r(z) = \mathbf{c}_r^* [z \mathbf{I} - \mathbf{A}_r]^{-1} \mathbf{b}_r$ with matrices

$$(3.3) \quad \mathbf{A}_r = (\mathbf{W}^* \mathbf{V})^{-1} \mathbf{W}^* \mathbf{A} \mathbf{V}, \quad \mathbf{b}_r = (\mathbf{W}^* \mathbf{V})^{-1} \mathbf{W}^* \mathbf{b}, \quad \mathbf{c}_r = \mathbf{V}^* \mathbf{c}$$

satisfies the Hermite interpolation conditions at each μ_j [28, Cor. 2.2]

$$(3.4) \quad H(\mu_j) = H_r(\mu_j), \quad H'(\mu_j) = H'_r(\mu_j), \quad j = 1, \dots, r$$

provided $\mathbf{W}^* \mathbf{V}$ is invertible. This interpolant satisfies the Meier-Luenberger conditions when the poles of H_r —the eigenvalues $\{\lambda_j\}_{j=1}^r$ of \mathbf{A}_r —are the interpolation points flipped across the imaginary axis; i.e., $\{-\bar{\lambda}_j\}_{j=1}^r = \{\mu_j\}_{j=1}^r$.

IRKA is a fixed point iteration that uses this Hermite interpolant to find a state-space reduced order model satisfying the Meier-Luenberger conditions. As summarized in Algorithm 3.1, given a set of interpolation points $\{\mu_j\}_{j=1}^r$ IRKA constructs a Hermite rational interpolant using (3.3) and then the poles of this rational interpolant $\{\lambda_j\}_{j=1}^r$ provide the new interpolation points for the next step, $\mu_j = -\bar{\lambda}_j$. When

this iteration converges, the reduced order model \widehat{H}_r satisfies the Meier-Luenberger conditions; moreover \widehat{H}_r is a local minimizer as local maximizers are repellent [7, subsec. 7.4.2]. Although IRKA often-times converges in practice, there are only limited cases where convergence is guaranteed [24] and examples exist where this fixed point iteration does not converge [7, subsec. 7.4.2]. For large scale model reduction, the cost of IRKA is dominated by the linear solves in (3.1) and (3.2). There are several modifications to IRKA that mitigate the cost of these linear solves by, for example, using inexact linear solves [8, 9], recycling information between iterations [1], and constructing local approximations of the full order model [17].

3.2. TF-IRKA. A critical limitation of IRKA is the need for a state-space representation of H for constructing the rational Krylov subspaces \mathcal{V} and \mathcal{W} used to build the rational interpolant reduced order model. Transfer function IRKA (TF-IRKA) [6] removes this constraint by constructing the reduced order model using a Loewner based approach following the work of Anderson and Antoulas [2]. Given a set of interpolation points $\{\mu_j\}_{j=1}^r$, TF-IRKA builds a Hermite interpolant $H_r(z) = \mathbf{c}_r^* [z\mathbf{E}_r - \mathbf{A}_r]^{-1} \mathbf{b}_r$ using evaluations of $H(\mu_j)$ and its derivative $H'(\mu_j)$ where

$$(3.5) \quad [\mathbf{A}_r]_{j,k} = \begin{cases} -\frac{\mu_j H(\mu_j) - \mu_k H(\mu_k)}{\mu_j - \mu_k}, & j \neq k; \\ -[zH(z)]'|_{z=\mu_j}, & j = k; \end{cases} \quad [\mathbf{E}_r]_{j,k} = \begin{cases} -\frac{H(\mu_j) - H(\mu_k)}{\mu_j - \mu_k}, & j \neq k; \\ -H'(\mu_j), & j = k; \end{cases}$$

and $[\mathbf{b}_r]_j = [\mathbf{c}_r]_j = H(\mu_j)$; here $[\mathbf{A}]_{j,k}$ denotes the j, k th entry of \mathbf{A} . Then, as in IRKA, the interpolation points are updated in a fixed point iteration based on the poles of H_r , in this case the generalized eigenvalues λ of $\mathbf{A}_r, \mathbf{E}_r$; e.g., $\mathbf{A}_r \mathbf{x} = \lambda \mathbf{E}_r \mathbf{x}$. When H has a state-space representation, the iterations of IRKA and TF-IRKA are identical in exact arithmetic.

3.3. QuadVF. An alternative approach taken by Quadrature-based Vector Fitting (QuadVF) [23] is to approximate the \mathcal{H}_2 norm using a quadrature rule and then solve the resulting weighted least squares rational approximation problem. QuadVF uses Boyd/Clelland-Curtis quadrature rule [14] using n evaluations of H plus its limit at $\pm\infty$ and includes a scaling parameter $L > 0$

$$(3.6) \quad \|H\|_{\mathcal{H}_2}^2 = \frac{1}{2\pi} \int_{-\infty}^{\infty} |H(i\omega)|^2 d\omega \approx \frac{|M_+[H]|^2 + |M_-[H]|^2}{4L(n+1)} + \sum_{j=1}^n w_j |H(z_j)|^2$$

$$(3.7) \quad w_j = \frac{L}{2(n+1) \sin^2(j\pi/(n+1))}, \quad z_j = iL \cot\left(\frac{j\pi}{n+1}\right), \quad M_{\pm}[H] = \lim_{\omega \rightarrow \pm\infty} i\omega H(i\omega).$$

This yields a diagonally weighted least squares rational approximation problem

$$(3.8) \quad \min_{H_r \in \mathcal{R}_r^+(\mathbb{R})} \left\| \begin{bmatrix} \sqrt{w_1} \\ \vdots \\ \sqrt{w_n} \\ \sqrt{w_+} \\ \sqrt{w_-} \end{bmatrix} \left(\begin{bmatrix} H(z_1) \\ \vdots \\ H(z_n) \\ M_+[H] \\ M_-[H] \end{bmatrix} - \begin{bmatrix} H_r(z_1) \\ \vdots \\ H_r(z_n) \\ M_+[H_r] \\ M_-[H_r] \end{bmatrix} \right) \right\|_2; \quad w_{\pm} = \frac{1}{4L(n+1)}$$

that is solved using a modification of Vector Fitting [29]. By using an approximate \mathcal{H}_2 -norm the reduced order model is necessarily suboptimal, but when n is sufficiently large can provide a reduced order model with small residual norm $\|H - H_r\|_{\mathcal{H}_2}$.

4. Projected Nonlinear Least Squares. Our approach for \mathcal{H}_2 -optimal model reduction extends the *projected nonlinear least squares* framework introduced by Hokanson for finite-dimensional problems [30]. In its original presentation, given a nonlinear least squares problem

$$(4.1) \quad \min_{\boldsymbol{\theta} \in \mathbb{R}^q} \|\mathbf{f}(\boldsymbol{\theta}) - \tilde{\mathbf{y}}\|_2^2 \quad \mathbf{f} : \mathbb{R}^q \rightarrow \mathbb{C}^n$$

this framework solves a series of projected problems, cf. [30, eq. (2)]

$$(4.2) \quad \hat{\boldsymbol{\theta}}^\ell := \operatorname{argmin}_{\boldsymbol{\theta} \in \mathbb{R}^q} \|\mathbf{P}_{\mathcal{W}_\ell}[\mathbf{f}(\boldsymbol{\theta}) - \mathbf{y}]\|_2^2 = \operatorname{argmin}_{\boldsymbol{\theta} \in \mathbb{R}^q} \|\mathbf{W}_\ell^*[\mathbf{f}(\boldsymbol{\theta}) - \mathbf{y}]\|_2^2$$

where $\mathbf{P}_{\mathcal{W}_\ell}$ is an orthogonal projector onto $\mathcal{W}_\ell \subset \mathbb{C}^n$ with orthonormal basis $\mathbf{W}_\ell \in \mathbb{C}^{n \times m_\ell}$ so that $\mathbf{P}_{\mathcal{W}_\ell} = \mathbf{W}_\ell \mathbf{W}_\ell^*$. Then by choosing subspaces \mathcal{W}_ℓ such that the largest subspace angle between \mathcal{W}_ℓ and the range of the Jacobian of $\mathbf{f}(\boldsymbol{\theta}^\ell)$ is small, we obtain an accurate solution the original problem (4.1). The advantage of this approach is that at each step we solve a nonlinear least squares problem of small dimension $m_\ell \ll n$. A caveat though is we must be able to evaluate the inner product $\mathbf{W}_\ell^* \mathbf{f}(\boldsymbol{\theta})$ inexpensively.

Applying this framework to \mathcal{H}_2 -optimal model reduction converts an infinite-dimensional optimization problem into a sequence of finite dimensional nonlinear least squares problems with the reproducing kernel structure of \mathcal{H}_2 providing the requisite inexpensive inner product. In the following subsections we build the projector for the \mathcal{H}_2 problem (subsection 4.1) and apply Lemma 1.1 to identify the desired range of the projector (subsection 4.2). Since our choice of projector precludes exact containment, we quantify the error introduced in terms of the subspace angle (subsection 4.3) and show this error can be made arbitrarily small (subsection 4.4).

4.1. Projection. Here we construct the projector $P(\boldsymbol{\mu})$ to be an orthogonal projector onto the subspace $\mathcal{V}(\boldsymbol{\mu})$ that spans the kernel vectors $v[\mu_k]$ (2.5):

$$(4.3) \quad \mathcal{V}(\boldsymbol{\mu}) := \operatorname{Span}\{v[\mu_k]\}_{k=1}^n \subset \mathcal{H}_2; \quad \boldsymbol{\mu} \in \mathbb{C}_+^n := \{\mathbf{z} \in \mathbb{C}^n \mid \operatorname{Re} z_k > 0\}.$$

To build this projector, we first define the linear operator $V(\boldsymbol{\mu}) : \mathbb{C}^n \rightarrow \mathcal{V}(\boldsymbol{\mu}) \subset \mathcal{H}_2$ and its adjoint $V(\boldsymbol{\mu})^* : \mathcal{H}_2 \rightarrow \mathbb{C}^n$,

$$(4.4) \quad V(\boldsymbol{\mu})\mathbf{c} = \sum_{k=1}^n c_k v[\mu_k], \quad V(\boldsymbol{\mu})^* H = \begin{bmatrix} \langle v[\mu_1], H \rangle_{\mathcal{H}_2} \\ \vdots \\ \langle v[\mu_n], H \rangle_{\mathcal{H}_2} \end{bmatrix} = \begin{bmatrix} H(\mu_1) \\ \vdots \\ H(\mu_n) \end{bmatrix} =: H(\boldsymbol{\mu})$$

Above we have invoked the kernel identity (2.6) to evaluate the adjoint. These two operators $V(\boldsymbol{\mu})$ and $V(\boldsymbol{\mu})^*$ satisfy the adjoint identity:

$$(4.5) \quad \langle V(\boldsymbol{\mu})\mathbf{c}, H \rangle_{\mathcal{H}_2} = \sum_{k=1}^n \overline{c_k} \langle v[\mu_k], H \rangle_{\mathcal{H}_2} = \mathbf{c}^* H(\boldsymbol{\mu}) = \langle \mathbf{c}, V(\boldsymbol{\mu})^* H \rangle_{\mathbb{C}^n}.$$

We now construct the orthogonal projector $P(\boldsymbol{\mu}) : \mathcal{H}_2 \rightarrow \mathcal{V}(\boldsymbol{\mu})$ as

$$(4.6) \quad P(\boldsymbol{\mu}) := V(\boldsymbol{\mu})[V(\boldsymbol{\mu})^* V(\boldsymbol{\mu})]^{-1} V(\boldsymbol{\mu})^* = V(\boldsymbol{\mu})\mathbf{M}(\boldsymbol{\mu})^{-1} V(\boldsymbol{\mu})^*$$

where $\mathbf{M}(\boldsymbol{\mu})$ is the positive definite Cauchy matrix

$$(4.7) \quad [\mathbf{M}(\boldsymbol{\mu})]_{j,k} := \langle v[\mu_j], v[\mu_k] \rangle_{\mathcal{H}_2} = (\mu_j + \overline{\mu_k})^{-1}.$$

With these definitions, the projected norm can be evaluated as a weighted Euclidean norm of the difference between samples of H and H_r evaluated at $\boldsymbol{\mu}$:

$$\begin{aligned}
 \|P(\boldsymbol{\mu})[H - H_r]\|_{\mathcal{H}_2}^2 &= \langle V(\boldsymbol{\mu})\mathbf{M}(\boldsymbol{\mu})^{-1}V(\boldsymbol{\mu})^*[H - H_r], [H - H_r] \rangle_{\mathcal{H}_2} \\
 &= \langle \mathbf{M}(\boldsymbol{\mu})^{-\frac{1}{2}}V(\boldsymbol{\mu})^*[H - H_r], \mathbf{M}(\boldsymbol{\mu})^{-\frac{1}{2}}V(\boldsymbol{\mu})^*[H - H_r] \rangle_{\mathcal{H}_2} \\
 (4.8) \quad &= \langle \mathbf{M}(\boldsymbol{\mu})^{-\frac{1}{2}}[H(\boldsymbol{\mu}) - H_r(\boldsymbol{\mu})], \mathbf{M}(\boldsymbol{\mu})^{-\frac{1}{2}}[H(\boldsymbol{\mu}) - H_r(\boldsymbol{\mu})] \rangle_{\mathbb{C}^n} \\
 &= \|\mathbf{M}(\boldsymbol{\mu})^{-\frac{1}{2}}[H(\boldsymbol{\mu}) - H_r(\boldsymbol{\mu})]\|_2^2;
 \end{aligned}$$

where $\mathbf{M}(\boldsymbol{\mu})^{-\frac{1}{2}}$ is a matrix square root such that $\mathbf{M}(\boldsymbol{\mu})^{-\frac{1}{2}}*\mathbf{M}(\boldsymbol{\mu})^{-\frac{1}{2}} = \mathbf{M}(\boldsymbol{\mu})^{-1}$.

4.2. First Order Necessary Conditions. We now revisit Lemma 1.1 to derive conditions under which a local optimizer of the projected problem is also a local optimizer of the original problem. For simplicity we consider a parameterization of $\mathcal{R}_r^+(\mathbb{C})$ in terms of poles and residues (cf. (2.7))

$$(4.9) \quad \widehat{\boldsymbol{\lambda}}, \widehat{\boldsymbol{\rho}} := \underset{\substack{\boldsymbol{\lambda}, \boldsymbol{\rho} \in \mathbb{C}^r \\ \text{Re } \lambda_k < 0}}{\text{argmin}} \|H - H_r(\cdot; \boldsymbol{\lambda}, \boldsymbol{\rho})\|_{\mathcal{H}_2}^2, \quad H_r(z; \boldsymbol{\lambda}, \boldsymbol{\rho}) := \sum_{k=1}^r \rho_k v[-\overline{\lambda}_k](z)$$

As $\boldsymbol{\lambda}$ and $\boldsymbol{\rho}$ are contained in an open set, we can apply Lemma 1.1. Thus if $\widehat{\boldsymbol{\lambda}}, \widehat{\boldsymbol{\rho}}$ are local optimizers of the projected version of (4.9), and $P(\boldsymbol{\mu}) \supseteq \mathcal{T}(\widehat{\boldsymbol{\lambda}}, \widehat{\boldsymbol{\rho}})$ where $\mathcal{T}(\widehat{\boldsymbol{\lambda}}, \widehat{\boldsymbol{\rho}})$ contains the derivatives with respect to this parameterization:

$$(4.10) \quad \mathcal{T}(\boldsymbol{\lambda}, \boldsymbol{\rho}) := \text{Span} \{ \rho_k v[-\overline{\lambda}_k]', i\rho_k v[-\overline{\lambda}_k]', v[-\overline{\lambda}_k], iv[-\overline{\lambda}_k] \}_{k=1}^r \subset \mathcal{H}_2,$$

then $\widehat{\boldsymbol{\lambda}}, \widehat{\boldsymbol{\rho}}$ are also local optimizers of the original problem (4.9). Note these the vectors in $\mathcal{T}(\boldsymbol{\lambda}, \boldsymbol{\rho})$ are precisely those that appear in the derivation the Meier-Luenberger conditions in (2.8)–(2.11). As the span contains all linear combinations, we denote this subspace using $\boldsymbol{\lambda}$ alone

$$(4.11) \quad \mathcal{T}(\boldsymbol{\lambda}) := \text{Span}\{v[-\overline{\lambda}_j], v[-\overline{\lambda}_j]'\}_{j=1}^r \supseteq \mathcal{T}(\boldsymbol{\lambda}, \boldsymbol{\rho})$$

with equality holding when $\rho_k \neq 0$. Finally, as $\mathcal{R}_r^+(\mathbb{R}) \subset \mathcal{R}_r^+(\mathbb{C})$, satisfying $P(\boldsymbol{\mu}) \supseteq \mathcal{T}(\boldsymbol{\lambda})$ is sufficient to apply Lemma 1.1 when $\mathcal{M} = \mathcal{R}_r^+(\mathbb{R})$.

4.3. Approximating Necessary Conditions. Unfortunately the construction of projector $P(\boldsymbol{\mu})$ precludes exactly satisfying the containment $\text{Range } P(\boldsymbol{\mu}) \supseteq \mathcal{T}(\boldsymbol{\lambda})$; $\mathcal{T}(\boldsymbol{\lambda})$ contains not only $v[-\overline{\lambda}_k]$, but $v[-\overline{\lambda}_k]'$ which is not in the range of $P(\boldsymbol{\mu})$. However if the range of $P(\boldsymbol{\mu})$ approximates $\mathcal{T}(\boldsymbol{\lambda})$ —as measured by the subspace angle—we are able to approximately satisfy the necessary conditions for the original problem.

Subspace angles on \mathcal{H}_2 generalize naturally from their finite dimensional analogue. Given two finite-dimensional subspaces $\mathcal{X} \subset \mathcal{H}_2$ and $\mathcal{Y} \subset \mathcal{H}_2$ of dimension m and n , the k th subspace angle ϕ_k between these subspaces \mathcal{X} and \mathcal{Y} is defined analogously to its finite-dimensional counterpart [12, eq. (2)]:

$$(4.12) \quad \cos \phi_k(\mathcal{X}, \mathcal{Y}) := \max_{\substack{X \in \mathcal{X} \\ \|X\|_{\mathcal{H}_2}=1 \\ \langle X_j, X \rangle_{\mathcal{H}_2}=0 \\ j < k}} \max_{\substack{Y \in \mathcal{Y} \\ \|Y\|_{\mathcal{H}_2}=1 \\ \langle Y_j, Y \rangle_{\mathcal{H}_2}=0 \\ j < k}} \langle X, Y \rangle_{\mathcal{H}_2}, \quad \phi_1 \leq \phi_2 \leq \dots \leq \phi_{\min(m,n)},$$

where $X_k \in \mathcal{X}$ and $Y_k \in \mathcal{Y}$ are the arguments that yield ϕ_k . Given unitary basis operators $B_{\mathcal{X}} : \mathbb{C}^m \rightarrow \mathcal{X}$ and $B_{\mathcal{Y}} : \mathbb{C}^n \rightarrow \mathcal{Y}$, we can compute the subspace angles via the singular values of a finite dimensional matrix

$$(4.13) \quad \cos \phi_k(\mathcal{X}, \mathcal{Y}) = \sigma_k(B_{\mathcal{X}}^* B_{\mathcal{Y}}); \quad B_{\mathcal{X}}^* B_{\mathcal{Y}} \in \mathbb{C}^{m \times n}$$

where σ_k denotes the k th singular value in descending order; cf. [12, Thm. 1].

For the purpose of analysis and computing the subspace angle, we introduce the orthogonal projector $Q(\boldsymbol{\lambda}) : \mathcal{H}_2 \rightarrow \mathcal{T}(\boldsymbol{\lambda})$. Defining the operator $V'(\boldsymbol{\mu}) : \mathbb{C}^n \rightarrow \mathcal{H}_2$ analogously to $V(\boldsymbol{\mu})$ using $v[\mu]'$ in place of $v[\mu]$, we note

$$(4.14) \quad V'(\boldsymbol{\mu})\mathbf{c} := \sum_{k=1}^n c_k v[\mu_k]', \quad V'(\boldsymbol{\mu})^* H := \begin{bmatrix} \langle v[\mu_1]', H \rangle_{\mathcal{H}_2} \\ \vdots \\ \langle v[\mu_n]', H \rangle_{\mathcal{H}_2} \end{bmatrix} = \begin{bmatrix} -H'(\mu_1) \\ \vdots \\ -H'(\mu_n) \end{bmatrix}$$

where the last equality follows from integration by parts. Using this definition, we write the projector $Q(\boldsymbol{\lambda})$ as

$$(4.15) \quad Q(\boldsymbol{\lambda}) := [V(-\bar{\boldsymbol{\lambda}}) \quad V'(-\bar{\boldsymbol{\lambda}})] \begin{bmatrix} V(-\bar{\boldsymbol{\lambda}})^* V(-\bar{\boldsymbol{\lambda}}) & V(-\bar{\boldsymbol{\lambda}})^* V'(-\bar{\boldsymbol{\lambda}}) \\ V'(-\bar{\boldsymbol{\lambda}})^* V(-\bar{\boldsymbol{\lambda}}) & V'(-\bar{\boldsymbol{\lambda}})^* V'(-\bar{\boldsymbol{\lambda}}) \end{bmatrix}^{-1} \begin{bmatrix} V(-\bar{\boldsymbol{\lambda}})^* \\ V'(-\bar{\boldsymbol{\lambda}})^* \end{bmatrix}.$$

We denote this interior matrix as $\widehat{\mathbf{M}}(\boldsymbol{\lambda})$:

$$(4.16) \quad \widehat{\mathbf{M}}(\boldsymbol{\lambda}) := \begin{bmatrix} V(-\bar{\boldsymbol{\lambda}})^* V(-\bar{\boldsymbol{\lambda}}) & V(-\bar{\boldsymbol{\lambda}})^* V'(-\bar{\boldsymbol{\lambda}}) \\ V'(-\bar{\boldsymbol{\lambda}})^* V(-\bar{\boldsymbol{\lambda}}) & V'(-\bar{\boldsymbol{\lambda}})^* V'(-\bar{\boldsymbol{\lambda}}) \end{bmatrix} \in \mathbb{C}^{(2r) \times (2r)},$$

whose blocks are

$$(4.17) \quad [V(-\bar{\boldsymbol{\lambda}})^* V(-\bar{\boldsymbol{\lambda}})]_{j,k} = \langle v[-\bar{\lambda}_j], v[-\bar{\lambda}_k] \rangle_{\mathcal{H}_2} = -(\bar{\lambda}_j + \lambda_k)^{-1};$$

$$(4.18) \quad [V(-\bar{\boldsymbol{\lambda}})^* V'(-\bar{\boldsymbol{\lambda}})]_{j,k} = \langle v[-\bar{\lambda}_j], v[-\bar{\lambda}_k]' \rangle_{\mathcal{H}_2} = -(\bar{\lambda}_j + \lambda_k)^{-2};$$

$$(4.19) \quad [V'(-\bar{\boldsymbol{\lambda}})^* V'(-\bar{\boldsymbol{\lambda}})]_{j,k} = \langle v[-\bar{\lambda}_j]', v[-\bar{\lambda}_k]' \rangle_{\mathcal{H}_2} = -2(\bar{\lambda}_j + \lambda_k)^{-3}.$$

This projector $Q(\boldsymbol{\lambda})$ provides an alternative interpretation of the optimality conditions (1.6) and (1.7). First note the original statement in (1.6) can be rewritten using the projector $Q(\boldsymbol{\lambda})$ to construct elements of $\mathcal{T}(\boldsymbol{\lambda})$

$$(4.20) \quad \langle H - H_r, T \rangle_{\mathcal{H}_2} = 0 \quad \forall T \in \mathcal{T}(\boldsymbol{\lambda}) \quad \Leftrightarrow \quad \langle H - H_r, Q(\boldsymbol{\lambda})F \rangle_{\mathcal{H}_2} = 0 \quad \forall F \in \mathcal{H}_2.$$

After moving $Q(\boldsymbol{\lambda})$ into the left hand argument, this second statement must be true for $F = Q(\boldsymbol{\lambda})[H - H_r]$; this choice is also sufficient since this F maximizes the inner product up to a scalar multiple. Hence,

$$(4.21) \quad \langle H - H_r, T \rangle_{\mathcal{H}_2} = 0 \quad \forall T \in \mathcal{T}(\boldsymbol{\lambda}) \quad \Leftrightarrow \quad \|Q(\boldsymbol{\lambda})[H - H_r]\|_{\mathcal{H}_2} = 0.$$

Applying the same argument to the projected problem, the local optimality conditions in (1.6) and (1.7) are equivalently

$$(4.22) \quad \|Q(\widehat{\boldsymbol{\lambda}})[H - H_r(\cdot; \widehat{\boldsymbol{\lambda}}, \widehat{\boldsymbol{\rho}})]\|_{\mathcal{H}_2} = 0 \quad (\text{original}),$$

$$(4.23) \quad \|Q(\widehat{\boldsymbol{\lambda}})P(\boldsymbol{\mu})[H - H_r(\cdot; \widehat{\boldsymbol{\lambda}}, \widehat{\boldsymbol{\rho}})]\|_{\mathcal{H}_2} = 0 \quad (\text{projected}).$$

The following theorem generalizes Lemma 1.1 when $\text{Range } P(\boldsymbol{\mu}) \not\subseteq \mathcal{T}(\boldsymbol{\lambda})$.

THEOREM 4.1. *Suppose $H_r(\cdot; \widehat{\boldsymbol{\lambda}}, \widehat{\boldsymbol{\rho}})$ is a local minimizer of the projected problem with $\|Q(\widehat{\boldsymbol{\lambda}})P(\boldsymbol{\mu})[H - H_r(\cdot; \widehat{\boldsymbol{\lambda}}, \widehat{\boldsymbol{\rho}})]\|_{\mathcal{H}_2} = 0$. Then $H_r(\cdot; \widehat{\boldsymbol{\lambda}}, \widehat{\boldsymbol{\rho}})$ satisfies the first order optimality conditions for the original problem (4.9) with error*

$$(4.24) \quad \|Q(\widehat{\boldsymbol{\lambda}})[H - H_r(\cdot; \widehat{\boldsymbol{\lambda}}, \widehat{\boldsymbol{\rho}})]\|_{\mathcal{H}_2} \leq \|H - H_r(\cdot; \widehat{\boldsymbol{\lambda}}, \widehat{\boldsymbol{\rho}})\|_{\mathcal{H}_2} \sin \phi_{\max}(\mathcal{V}(\boldsymbol{\mu}), \mathcal{T}(\widehat{\boldsymbol{\lambda}})).$$

Proof. Inserting the identity $I = I - P(\boldsymbol{\mu}) + P(\boldsymbol{\mu})$ into the left hand side we have

$$(4.25) \quad \|Q(\widehat{\boldsymbol{\lambda}})[H - H_r(\cdot; \widehat{\boldsymbol{\lambda}}, \widehat{\boldsymbol{\rho}})]\|_{\mathcal{H}_2} \leq \\ \|Q(\widehat{\boldsymbol{\lambda}})(I - P(\boldsymbol{\mu}))[H - H_r(\cdot; \widehat{\boldsymbol{\lambda}}, \widehat{\boldsymbol{\rho}})]\|_{\mathcal{H}_2} + \|Q(\widehat{\boldsymbol{\lambda}})P(\boldsymbol{\mu})[H - H_r(\cdot; \widehat{\boldsymbol{\lambda}}, \widehat{\boldsymbol{\rho}})]\|_{\mathcal{H}_2}.$$

The second term is zero since $H_r(\cdot; \widehat{\boldsymbol{\lambda}}, \widehat{\boldsymbol{\rho}})$ satisfies the local optimality conditions of the projected problem in (4.23). Then bounding this quantity using the induced \mathcal{H}_2 -norm yields

$$(4.26) \quad \|Q(\widehat{\boldsymbol{\lambda}})[H - H_r(\cdot; \widehat{\boldsymbol{\lambda}}, \widehat{\boldsymbol{\rho}})]\|_{\mathcal{H}_2} \leq \|Q(\widehat{\boldsymbol{\lambda}})(I - P(\boldsymbol{\mu}))\|_{\mathcal{H}_2} \|H - H_r(\cdot; \widehat{\boldsymbol{\lambda}}, \widehat{\boldsymbol{\rho}})\|_{\mathcal{H}_2}.$$

By definition, the first term on the right is the largest subspace angle between $\mathcal{V}(\boldsymbol{\mu})$ and $\mathcal{T}(\widehat{\boldsymbol{\lambda}})$ [12, eq. (13)]

$$(4.27) \quad \|Q(\widehat{\boldsymbol{\lambda}})(I - P(\boldsymbol{\mu}))\|_{\mathcal{H}_2} = \sin \phi_{\max}(\mathcal{V}(\boldsymbol{\mu}), \mathcal{T}(\widehat{\boldsymbol{\lambda}})). \quad \square$$

To compute this subspace angle, we introduce the unitary basis operators for Range $P(\boldsymbol{\mu}) = \mathcal{V}(\boldsymbol{\mu})$ and Range $Q(\boldsymbol{\lambda}) = \mathcal{T}(\boldsymbol{\lambda})$

$$(4.28) \quad B_{\mathcal{V}(\boldsymbol{\mu})} : \mathbb{C}^n \rightarrow \mathcal{V}(\boldsymbol{\mu}) \quad B_{\mathcal{V}(\boldsymbol{\mu})} := V(\boldsymbol{\mu})\mathbf{M}(\boldsymbol{\mu})^{-\frac{1}{2}},$$

$$(4.29) \quad B_{\mathcal{T}(\boldsymbol{\lambda})} : \mathbb{C}^{2r} \rightarrow \mathcal{M}(\boldsymbol{\lambda}) \quad B_{\mathcal{T}(\boldsymbol{\lambda})} := [V(-\bar{\boldsymbol{\lambda}}) \quad V'(-\bar{\boldsymbol{\lambda}})] \widehat{\mathbf{M}}(\boldsymbol{\lambda})^{-\frac{1}{2}}.$$

Then the largest subspace angle between $\mathcal{V}(\boldsymbol{\mu})$ and $\mathcal{T}(\boldsymbol{\lambda})$ is

$$(4.30) \quad \cos \phi_{\max}(\mathcal{T}(\boldsymbol{\lambda}), \mathcal{V}(\boldsymbol{\mu})) = \sigma_{\min}(B_{\mathcal{V}(\boldsymbol{\mu})}^* B_{\mathcal{T}(\boldsymbol{\lambda})})$$

where σ_{\min} denotes the smallest singular value and

$$(4.31) \quad B_{\mathcal{V}(\boldsymbol{\mu})}^* B_{\mathcal{T}(\boldsymbol{\lambda})} = \mathbf{M}(\boldsymbol{\mu})^{-\frac{1}{2}} [V(\boldsymbol{\mu})^* V(-\bar{\boldsymbol{\lambda}}) \quad V(\boldsymbol{\mu})^* V'(-\bar{\boldsymbol{\lambda}})] \widehat{\mathbf{M}}(\boldsymbol{\lambda})^{-\frac{1}{2}} \in \mathbb{C}^{n \times (2r)}.$$

4.4. Finite-Difference Subspace. Although we cannot have exact containment of $\mathcal{T}(\boldsymbol{\lambda})$ inside $\mathcal{V}(\boldsymbol{\mu})$, we can get arbitrarily close. To provide an intuition of how this can happen, note that as a derivative, $v[\boldsymbol{\mu}]'$ can be approximated by a finite-difference for some small complex δ :

$$(4.32) \quad v[\boldsymbol{\mu}]' \approx \frac{v[\boldsymbol{\mu} + \delta] - v[\boldsymbol{\mu} - \delta]}{2|\delta|} \in \mathcal{V}([\boldsymbol{\mu} - \delta, \boldsymbol{\mu} + \delta]).$$

In the same spirit, the following theorem shows that the subspace $\mathcal{V}(\boldsymbol{\mu})$ with μ_j clustering near $-\bar{\lambda}$ can approximate $\mathcal{T}(\boldsymbol{\lambda})$ to arbitrary accuracy.

THEOREM 4.2. *Let $\mathcal{V}(\boldsymbol{\mu})$ be a n -dimensional subspace of \mathcal{H}_2 with $\boldsymbol{\mu} \in \mathbb{C}_+^n$ as defined in (4.4) where $\boldsymbol{\mu}$ are distinct and let $\mathcal{T}(\boldsymbol{\lambda})$ be a $2r$ -dimensional subspace of \mathcal{H}_2 with $\boldsymbol{\lambda} \in \mathbb{C}_-^r$ as defined in (4.11) where $\boldsymbol{\lambda}$ are distinct. If for each λ_k , there exist entries of $\boldsymbol{\mu}$ denoted $\mu_{k,1}$, $\mu_{k,2}$, and $\mu_{k,3}$ where $|\mu_{k,i} + \bar{\lambda}_k| \leq \epsilon$ for $i = 1, 2, 3$ and no entry $\mu_{k,i}$ is repeated, then there exists a constant C independent of ϵ such that*

$$(4.33) \quad \sin \phi_{\max}(\mathcal{T}(\boldsymbol{\lambda}), \mathcal{V}(\boldsymbol{\mu})) \leq C\epsilon.$$

Due to the highly technical nature of this proof, it has been placed in the appendix.

5. Outer Loop: Sampling the Full Order Model. Having shown in the previous section that the local optimality conditions can be satisfied to arbitrary accuracy using the projected nonlinear least squares framework, we now design an efficient algorithm constructing a sequence of projectors $\{P(\boldsymbol{\mu}^\ell)\}_{\ell=0}^\infty$ to solve the \mathcal{H}_2 -optimal model reduction problem. As we assume the dominant cost is evaluating the full order model—namely evaluating $H(z)$ —we choose a nested sequence of projectors

$$(5.1) \quad \text{Range } P(\boldsymbol{\mu}^\ell) \subset \text{Range } P(\boldsymbol{\mu}^{\ell+1}) \quad \boldsymbol{\mu}^{\ell+1} := [\boldsymbol{\mu}^\ell \quad \mu_\star^\ell]$$

to reuse previous evaluations of $H(\mu_j)$. In this section we provide a simple heuristic for choosing a new interpolation point μ_\star^ℓ based on the poles of the current iterate

$$(5.2) \quad \widehat{H}_r^\ell := \underset{H_r \in \mathcal{R}_r^+(\mathbb{R})}{\text{argmin}} \|P(\boldsymbol{\mu}^\ell)[H - H_r]\|_{\mathcal{H}_2}.$$

We are able to prove that when this heuristic generates reduced order models \widehat{H}_r^ℓ converging to \widehat{H}_r , that \widehat{H}_r is a local optimizer of the original problem. We then modify this iteration slightly to address numerical concerns.

5.1. Selecting Interpolation Points. Much like IRKA chooses new interpolation points that are the poles of \widehat{H}_r^ℓ flipped across the imaginary axis, we select a new interpolation point μ_\star^ℓ to append from the poles of \widehat{H}_r^ℓ flipped across the imaginary axis. However rather than appending all r poles of \widehat{H}_r^ℓ , we choose to append only one—namely, the one that is furthest away from $\mathcal{V}(\boldsymbol{\mu})$ in terms of the subspace angle

$$(5.3) \quad \mu_\star^\ell := -\overline{\lambda}_\star^\ell \quad \text{where} \quad \lambda_\star^\ell := \underset{\lambda \in \boldsymbol{\lambda}(\widehat{H}_r^\ell)}{\text{argmax}} \sin \phi_{\max}(\mathcal{V}(\boldsymbol{\mu}^\ell), \mathcal{T}(\lambda))$$

and $\boldsymbol{\lambda}(H)$ denotes the poles of H . These subspace angles can be computed via (4.30)

$$(5.4) \quad \cos \phi_{\max}(\mathcal{V}(\boldsymbol{\mu}), \mathcal{T}(\lambda)) = \sigma_{\min} \left(\mathbf{M}(\boldsymbol{\mu})^{-\frac{1}{2}} \begin{bmatrix} \frac{1}{\mu_1 - \lambda} & \frac{1}{(\mu_1 - \lambda)^2} \\ \vdots & \vdots \\ \frac{1}{\mu_n - \lambda} & \frac{1}{(\mu_n - \lambda)^2} \end{bmatrix} \begin{bmatrix} -1 & \frac{1}{(\overline{\lambda} + \lambda)^2} \\ \frac{\overline{\lambda} + \lambda}{1} & \frac{-2}{(\overline{\lambda} + \lambda)^3} \end{bmatrix}^{-\frac{1}{2}} \right).$$

Evaluating this subspace angle is inexpensive, taking only $\mathcal{O}(n^2)$ operations, and can reuse the factorization of $\mathbf{M}(\boldsymbol{\mu})$ computed as part of solving the nonlinear least squares problem as discussed in subsection 6.5. In addition to being inexpensive, this subspace update rule yields a sequence of projected reduced order models \widehat{H}_r^ℓ which, when they converge, converge to a local optimizer of the original problem under mild conditions.

THEOREM 5.1. *Let $H \in \mathcal{H}_2$ and n_0, r be a positive integers where $n_0 \geq 2r$. Given an initial $\boldsymbol{\mu}^0 \in \mathbb{C}_+^{n_0}$ with distinct entires, let $\boldsymbol{\mu}^\ell$ and \widehat{H}_r^ℓ be generated by the iteration*

$$(5.5) \quad \widehat{H}_r^\ell := \underset{H_r \in \mathcal{R}_r^+(\mathbb{C})}{\text{argmin}} \|P(\boldsymbol{\mu}^\ell)[H - H_r]\|_{\mathcal{H}_2} \quad \text{with} \quad \|Q(\boldsymbol{\lambda}(\widehat{H}_r^\ell))P(\boldsymbol{\mu}^\ell)[H - \widehat{H}_r^\ell]\|_{\mathcal{H}_2} = 0;$$

$$(5.6) \quad \boldsymbol{\mu}^{\ell+1} := [\boldsymbol{\mu}^\ell \quad \mu_\star^\ell], \quad \mu_\star^\ell := -\overline{\lambda}_\star^\ell, \quad \lambda_\star^\ell := \underset{\lambda \in \boldsymbol{\lambda}(\widehat{H}_r^\ell)}{\text{argmax}} \sin \phi_{\max}(\mathcal{V}(\boldsymbol{\mu}^\ell), \mathcal{T}(\lambda)).$$

If the sequence $\{\mu_\star^\ell\}_{\ell=0}^\infty$ has distinct, bounded entries and $\widehat{H}_r^\ell \rightarrow \widehat{H}_r \in \mathcal{H}_2$ where \widehat{H}_r has r distinct poles, then \widehat{H}_r satisfies the first order necessary conditions of the \mathcal{H}_2 problem (4.22); i.e., \widehat{H}_r satisfies the Meier-Luenberger conditions.

Algorithm 5.1 Projected Nonlinear Least Squares for Real \mathcal{H}_2 Model Reduction

Input : Real FOM $H \in \mathcal{H}_2$, order $r > 0$, initial samples $\boldsymbol{\mu}^0 \in \mathbb{C}_+^{n_0}$, tolerance $\tau > 0$
Output : Real ROM $H_r \in \mathcal{H}_2$

- 1 **for** $\ell = 0, 1, 2, \dots$ **do**
- 2 Set n to be the length of $\boldsymbol{\mu}^\ell$;
- 3 **if** $n < 2r$ **then** Set $r \leftarrow 2\lfloor n/4 \rfloor$ for only the next iteration ;
- 4 Solve projected problem: $\widehat{H}_r^\ell \leftarrow \operatorname{argmin}_{H_r \in \mathcal{R}_r^+(\mathbb{R})} \|P(\boldsymbol{\mu}^\ell)[H - H_r]\|_{\mathcal{H}_2}$;
- 5 **if** $\|\widehat{H}_r^\ell - \widehat{H}_r^{\ell-1}\|_{\mathcal{H}_2} < \tau$ **then break** ;
- 6 Compute poles of \widehat{H}_r^ℓ : $\boldsymbol{\lambda} \leftarrow \lambda(\widehat{H}_r^\ell) \subset \mathbb{C}_-^r$;
- 7 Using AAA, construct a degree- $(\widehat{r}, \widehat{r})$ rational approximation G of $\boldsymbol{\mu}, H(\boldsymbol{\mu})$;
- 8 Compute poles of G : $\boldsymbol{\nu} \leftarrow \lambda(G)$; flip into \mathbb{C}_-^r by $\nu_j \leftarrow -|\operatorname{Re} \nu_j| + \operatorname{Im} \nu_j$;
- 9 Order $\boldsymbol{\nu}$ to minimize $|\nu_j - \lambda_j|$ using the Kuhn-Munkres algorithm;
- 10 **if** $\lambda_j \notin \mathcal{F}(\boldsymbol{\mu})$ **then** set $\lambda_j \leftarrow \nu_j$;
- 11 Compute furthest pole: $\lambda_* \leftarrow \operatorname{argmax}_{\lambda \in \boldsymbol{\lambda}} \phi_{\max}(\mathcal{M}(\lambda), \mathcal{V}(\boldsymbol{\mu}))$;
- 12 **if** $\operatorname{Im} \lambda_* \neq 0$ **then** Update samples: $\boldsymbol{\mu}^{\ell+1} \leftarrow [\boldsymbol{\mu}^\ell \quad -\lambda_* \quad -\overline{\lambda_*}]$;
- 13 **else** Update samples: $\boldsymbol{\mu}^{\ell+1} \leftarrow [\boldsymbol{\mu}^\ell \quad -\lambda_*]$;

A full proof is provided in the appendix, but in brief, this result follows from the assumption that the samples $\{\mu_*^\ell\}_{\ell=0}^\infty$ are bounded. Thus this sequence has an accumulation point, which by construction is the pole $\widehat{\lambda}_k$ of \widehat{H}_r . Consequently by invoking Theorem 4.2, we know the subspace angle between $\mathcal{T}(\widehat{\lambda}_k)$ and $\mathcal{V}(\boldsymbol{\mu}^\ell)$ goes to zero and this implies the same for the remainder of the poles of \widehat{H}_r ; hence \widehat{H}_r satisfies the Meier-Luenberger conditions.

A notable case that does not satisfy the assumptions of this theorem occurs when $H \in \mathcal{R}_r^+(\mathbb{R})$. For this case, given any set of distinct samples $\boldsymbol{\mu} \in \mathbb{C}_+^n$ where $n \geq 2r$ we recover H exactly, namely $\widehat{H}_r = H$. Thus the poles of \widehat{H}_r^ℓ are always the same and the sequence $\{\mu_*^\ell\}_{\ell=0}^\infty$ violates the assumption of being distinct. However in this case, the iteration given in (5.5) and (5.6) still returns an optimal reduced order model.

Before concluding, we note there are a variety of other potential subspace update rules. For example, we could choose μ to minimize the subspace angle between the tangent subspace associated with the current iterate and the projection subspace,

$$(5.7) \quad \min_{\mu \in \mathbb{C}_+} \sin \phi_{\max}(\mathcal{T}(\boldsymbol{\lambda}(\widehat{H}_r^\ell)), \mathcal{V}(\boldsymbol{\mu}^\ell) \cup \mathcal{V}(\mu)).$$

However, unlike the update rule we propose (5.2), this is a nonconvex optimization problem and evaluating these subspace angles is both expensive and ill-conditioned.

5.2. Practical Algorithm. In numerical practice, we modify the iteration given in Theorem 5.1 as described in Algorithm 5.1.

5.2.1. Conjugate Samples. Since we assume that the full order model $H \in \mathcal{H}_2$ is real, we can evaluate $H(\mu)$ and $H(\overline{\mu})$ through only one evaluation of H as $\overline{H(\mu)} = H(\overline{\mu})$. Thus if μ_* is not on the real line, we automatically include its conjugate in line 12 which incurs no additional evaluation of H .

5.2.2. Intermediate Dimension. If the rational approximation problem is underdetermined, we choose an intermediate dimension for the reduced order model $\widehat{r} < r$ such that the rational approximation problem on line 4 exactly determined or overdetermined. We always pick an even order (cf. line 3) as odd real rational models must have a pole on the real line, but \widehat{H}_r may not.

5.2.3. Spurious Poles. The least squares rational approximation step on line 4 may yield a solution whose poles are spurious for our purposes. For example, a pole may be far away from existing samples; e.g., with $\text{Im } \mu_j \in [-1, 1]$, there could be a pole λ_k with $\text{Im } \lambda_k \approx 10^7$. In this case $(\mu_j - \lambda_k)^{-1}$ is small leading to inaccurate estimation of λ_k . Similarly, a pole λ_k may appear on the imaginary axis with $\text{Re } \lambda_k = 0$, an artifact of the box constraints introduced to ensure $H_r \in \mathcal{H}_2$ (see subsection 6.1). Without modification, a spurious pole can trigger a cascade leading the algorithm to fail: the subspace angle criteria on line 11 ensures these spurious poles are selected, causing $\mathbf{M}(\boldsymbol{\mu})$ to be ill-conditioned, and leading subsequent rational approximation steps to fail. To mitigate this failure mode we introduce a heuristic to identify and replace these spurious poles. We label poles as spurious if they fall outside of box containing $\boldsymbol{\mu}$ that has been enlarged by a factor of ten

$$(5.8) \quad \mathcal{F}(\boldsymbol{\mu}) := [-10 \max_{\mu \in \boldsymbol{\mu}} \text{Re } \mu, -0.1 \min_{\mu \in \boldsymbol{\mu}} \text{Re } \mu] \times i[10 \min_{\mu \in \boldsymbol{\mu}} \text{Im } \mu, 10 \max_{\mu \in \boldsymbol{\mu}} \text{Im } \mu] \subset \mathbb{C}_-.$$

Scaling by a factor of ten balances the need allow new interpolation points μ to extend beyond existing $\boldsymbol{\mu}$ while still identifying likely spurious poles. When a pole has been labeled spurious, we replace this pole with the corresponding pole from a AAA rational approximation as shown on line 10; note this AAA rational approximation was already constructed during the initialization of the rational approximation step (see subsection 6.4). Although the AAA poles are not optimal, in practice they are not spurious and provide relevant information about H . Although this alters the iteration presented in Theorem 5.1, this result still applies as if $\widehat{H}_r^\ell \rightarrow \widehat{H}_r$, eventually all poles lie in $\mathcal{F}(\boldsymbol{\mu})$ and this modification is inactive.

5.2.4. Termination Criteria. Here we terminate the algorithm when the difference between subsequent iterates measured in the \mathcal{H}_2 norm is small (line 5), choosing this norm to remove the effects of parameterization of H_r . Computing this quantity only requires $\mathcal{O}(r^3)$ operations using (2.4), Ideally based on Theorem 4.1, we would prefer to terminate when the subspace angle between $\mathcal{V}(\boldsymbol{\mu}^\ell)$ and $\mathcal{T}(\boldsymbol{\lambda}(\widehat{H}_r^\ell))$ is sufficiently small; unfortunately this quantity proves difficult to compute accurately.

6. Inner Loop: Constructing a Reduced Order Model. A critical component of our Projected \mathcal{H}_2 approach is the construction of a *weighted least squares rational approximant* on line 4 of Algorithm 5.1

$$(6.1) \quad \widehat{H}_r^\ell := \underset{H_r \in \mathcal{R}_r^+(\mathbb{R})}{\text{argmin}} \|P(\boldsymbol{\mu}^\ell)[H - H_r]\|_{\mathcal{H}_2} = \underset{H_r \in \mathcal{R}_r^+(\mathbb{R})}{\text{argmin}} \|\mathbf{M}(\boldsymbol{\mu}^\ell)^{-\frac{1}{2}}[H(\boldsymbol{\mu}^\ell) - H_r(\boldsymbol{\mu}^\ell)]\|_2.$$

In Theorem 4.2, an important assumption required for the outer loop to yield local optimizers was that these iterates \widehat{H}_r^ℓ are local optimizers of (6.1). Unfortunately, many popular rational fitting algorithms do not yield local optimizers for this problem. For example, Adaptive Anderson-Antoulas (AAA) [37] exactly interpolates at some μ_j and suboptimally approximates on the remainder. Both the Sanathanan-Koerner iteration [39] and Vector Fitting [29] have been shown, in general, to converge to rational approximants that do not satisfy the necessary conditions [41]. This lack of existing results motivates our development of a nonlinear least squares approach to solve this weighted rational approximation problem. Here we introduce a two-term partial fraction expansion of H_r to implicitly enforce the constraint that H_r is real and apply variable projection [26] to reduce the dimension of the optimization problem. Additional information about this approach appears in a companion manuscript [31].

6.1. Parameterization. To construct a rational approximation, we must first choose a parameterization of the space of real rational functions of degree $(r-1, r)$: $\mathcal{R}_r^+(\mathbb{R})$. As discussed in [31, sec. 3.4], naive approaches have significant drawbacks: parametrizing $\mathcal{R}_r^+(\mathbb{R})$ as a ratio of monomials rapidly leads to ill-conditioning and a pole-residue parameterization requires additional nonlinear constraints to ensure the rational function has a real representation. Instead, we use a two-term partial fraction expansion following [31, subsec. 4.2]:

$$(6.2) \quad H_r^{\text{PF}}(z; \mathbf{a}, \mathbf{b}) := \begin{cases} \sum_{k=1}^{\lfloor r/2 \rfloor} \frac{a_{2k}z + a_{2k-1}}{z^2 + b_{2k}z + b_{2k-1}}, & r \text{ even;} \\ \frac{a_r}{z + b_r} + \sum_{k=1}^{\lfloor r/2 \rfloor} \frac{a_{2k}z + a_{2k-1}}{z^2 + b_{2k}z + b_{2k-1}}, & r \text{ odd;} \end{cases} \quad \mathbf{a}, \mathbf{b} \in \mathbb{R}^r.$$

This parameterization has several advantages: it is (comparably) numerically stable, requires only $2r$ real parameters, and allows us to enforce $H_r^{\text{PF}} \in \mathcal{R}_r^+(\mathbb{R})$ through a box constraint. Recall $H_r^{\text{PF}} \in \mathcal{R}_r^+(\mathbb{R}) \subset \mathcal{H}_2$ if its poles are in the left half plane. As the poles of H_r^{PF} are $-b_{2k}/2 \pm \sqrt{b_{2k}^2/4 - b_{2k-1}}$ (and $-b_r$ if r is odd) it is both necessary and sufficient to require $b_k > 0$ for H_r^{PF} to be in $\mathcal{R}_r^+(\mathbb{R})$.

6.2. Variable Projection. Using this parameterization, we construct the rational approximant by solving the rational approximation problem (6.1)

$$(6.3) \quad \min_{\substack{\mathbf{a}, \mathbf{b} \in \mathbb{R}^r \\ b_k > 0}} \left\| \mathbf{M}(\boldsymbol{\mu})^{-\frac{1}{2}} [H(\boldsymbol{\mu}) - H_r^{\text{PF}}(\boldsymbol{\mu}; \mathbf{a}, \mathbf{b})] \right\|_2.$$

We write $H_r^{\text{PF}}(\boldsymbol{\mu}; \mathbf{a}, \mathbf{b})$ as the matrix-vector product $H_r^{\text{PF}}(\boldsymbol{\mu}; \mathbf{a}, \mathbf{b}) = \boldsymbol{\Theta}(\mathbf{b})\mathbf{a}$ where

$$(6.4) \quad \boldsymbol{\Theta}(\mathbf{b}) := \begin{cases} \begin{bmatrix} \boldsymbol{\Omega}([\mathbf{b}]_{1:2}) & \cdots & \boldsymbol{\Omega}([\mathbf{b}]_{r-1:r}) \end{bmatrix}, & r \text{ even;} \\ \begin{bmatrix} \boldsymbol{\Omega}([\mathbf{b}]_{1:2}) & \cdots & \boldsymbol{\Omega}([\mathbf{b}]_{r-2:r-1}) & (\boldsymbol{\mu} + b_r)^{-1} \end{bmatrix}, & r \text{ odd;} \end{cases}$$

$$(6.5) \quad \boldsymbol{\Omega} \left(\begin{bmatrix} b_1 \\ b_2 \end{bmatrix} \right) := \begin{bmatrix} \frac{\mu_1}{\mu_1^2 + b_2\mu_1 + b_1} & \frac{1}{\mu_1^2 + b_2\mu_1 + b_1} \\ \vdots & \vdots \\ \frac{\mu_n}{\mu_n^2 + b_2\mu_n + b_1} & \frac{1}{\mu_n^2 + b_2\mu_n + b_1} \end{bmatrix} \in \mathbb{C}^{n \times 2}.$$

This exposes the separable structure of (6.3), which for fixed \mathbf{b} yields a linear least squares problem in \mathbf{a} :

$$(6.6) \quad \min_{\substack{\mathbf{a}, \mathbf{b} \in \mathbb{R}^r \\ b_k > 0}} \left\| \mathbf{M}(\boldsymbol{\mu})^{-\frac{1}{2}} [H(\boldsymbol{\mu}) - \boldsymbol{\Theta}(\mathbf{b})\mathbf{a}] \right\|_2.$$

As the objective function involves the complex 2-norm, we recast this as an optimization problem over the real 2-norm by splitting into real and imaginary components

$$(6.7) \quad \min_{\substack{\mathbf{a}, \mathbf{b} \in \mathbb{R}^r \\ b_k > 0}} \left\| \begin{bmatrix} \text{Re } \mathbf{M}(\boldsymbol{\mu})^{-\frac{1}{2}} H(\boldsymbol{\mu}) \\ \text{Im } \mathbf{M}(\boldsymbol{\mu})^{-\frac{1}{2}} H(\boldsymbol{\mu}) \end{bmatrix} - \begin{bmatrix} \text{Re } \mathbf{M}(\boldsymbol{\mu})^{-\frac{1}{2}} \boldsymbol{\Theta}(\mathbf{b}) \\ \text{Im } \mathbf{M}(\boldsymbol{\mu})^{-\frac{1}{2}} \boldsymbol{\Theta}(\mathbf{b}) \end{bmatrix} \mathbf{a} \right\|_2.$$

Applying variable projection yields an equivalent optimization problem over \mathbf{b} alone

$$(6.8) \quad \min_{\substack{\mathbf{b} \in \mathbb{R}^r \\ b_k > 0}} \left\| \begin{bmatrix} \mathbf{I} - \begin{bmatrix} \text{Re } \mathbf{M}(\boldsymbol{\mu})^{-\frac{1}{2}} \boldsymbol{\Theta}(\mathbf{b}) \\ \text{Im } \mathbf{M}(\boldsymbol{\mu})^{-\frac{1}{2}} \boldsymbol{\Theta}(\mathbf{b}) \end{bmatrix} \begin{bmatrix} \text{Re } \mathbf{M}(\boldsymbol{\mu})^{-\frac{1}{2}} \boldsymbol{\Theta}(\mathbf{b}) \\ \text{Im } \mathbf{M}(\boldsymbol{\mu})^{-\frac{1}{2}} \boldsymbol{\Theta}(\mathbf{b}) \end{bmatrix}^+ \end{bmatrix} \begin{bmatrix} \text{Re } \mathbf{M}(\boldsymbol{\mu})^{-\frac{1}{2}} H(\boldsymbol{\mu}) \\ \text{Im } \mathbf{M}(\boldsymbol{\mu})^{-\frac{1}{2}} H(\boldsymbol{\mu}) \end{bmatrix} \right\|_2,$$

where $^+$ denotes the pseudoinverse.

Algorithm 6.1 Residual and Jacobian for Real Partial Fraction Parameterization

Input : Parameters $\mathbf{b} \in \mathbb{R}^r$, factorization $\mathbf{M}(\boldsymbol{\mu}) = \mathbf{P}\mathbf{L}\mathbf{D}\mathbf{L}^*\mathbf{P}^*$ (6.9)
Output : Residual $\mathbf{r} \in \mathbb{R}^{2n}$ and Jacobian $\mathbf{J} \in \mathbb{R}^{(2n) \times r}$

- 1 Form $\boldsymbol{\Theta} \leftarrow \boldsymbol{\Theta}(\mathbf{b})$ as given in (6.4);
- 2 Compute the short form QR decomposition $\underline{\mathbf{Q}}\underline{\mathbf{R}} \leftarrow \begin{bmatrix} \text{Re } \mathbf{D}^{-1/2} \mathbf{L}^{-*} \mathbf{P} \boldsymbol{\Theta} \\ \text{Im } \mathbf{D}^{-1/2} \mathbf{L}^{-*} \mathbf{P} \boldsymbol{\Theta} \end{bmatrix}$;
- 3 Define $\underline{\mathbf{h}} \leftarrow \begin{bmatrix} \text{Re } \mathbf{D}^{-1/2} \mathbf{L}^{-*} \mathbf{P} H(\boldsymbol{\mu}) \\ \text{Im } \mathbf{D}^{-1/2} \mathbf{L}^{-*} \mathbf{P} H(\boldsymbol{\mu}) \end{bmatrix}$;
- 4 Compute (real) residual $\mathbf{r} \leftarrow \underline{\mathbf{h}} - \underline{\mathbf{Q}}\underline{\mathbf{Q}}^\top \underline{\mathbf{h}}$;
- 5 Form complex residual $\mathbf{r} \leftarrow [\mathbf{r}]_{1:n} + i[\mathbf{r}]_{n+1:2n}$;
- 6 Compute linear coefficients $\mathbf{a} \leftarrow \underline{\mathbf{R}}^+ \underline{\mathbf{Q}}^\top \underline{\mathbf{h}}$;
- 7 **for** $k = 1, \dots, \lfloor r/2 \rfloor$ **do**
- 8 $\mathbf{d} \leftarrow \boldsymbol{\mu}^2 + b_{2k} \boldsymbol{\mu} + b_{2k-1}$;
- 9 $[\underline{\mathbf{K}}]_{:,2k-1} \leftarrow [\mathbf{I} - \underline{\mathbf{Q}}\underline{\mathbf{Q}}^\top] \begin{bmatrix} \text{Re } \mathbf{D}^{-1/2} \mathbf{L}^{-*} \mathbf{P} \text{diag}(\mathbf{d})^{-2} (a_{2k} \boldsymbol{\mu} + a_{2k-1}) \\ \text{Im } \mathbf{D}^{-1/2} \mathbf{L}^{-*} \mathbf{P} \text{diag}(\mathbf{d})^{-2} (a_{2k} \boldsymbol{\mu} + a_{2k-1}) \end{bmatrix}$;
- 10 $[\underline{\mathbf{K}}]_{:,2k} \leftarrow [\mathbf{I} - \underline{\mathbf{Q}}\underline{\mathbf{Q}}^\top] \begin{bmatrix} \text{Re } \mathbf{D}^{-1/2} \mathbf{L}^{-*} \mathbf{P} \text{diag}(\boldsymbol{\mu}) \text{diag}(\mathbf{d})^{-2} (a_{2k} \boldsymbol{\mu} + a_{2k-1}) \\ \text{Im } \mathbf{D}^{-1/2} \mathbf{L}^{-*} \mathbf{P} \text{diag}(\boldsymbol{\mu}) \text{diag}(\mathbf{d})^{-2} (a_{2k} \boldsymbol{\mu} + a_{2k-1}) \end{bmatrix}$;
- 11 $[\underline{\mathbf{L}}]_{:,2k-1} \leftarrow \underline{\mathbf{Q}}\underline{\mathbf{R}}^{+\top} \begin{bmatrix} \text{Re } \text{diag}(\mathbf{d})^{-2*} \mathbf{P}^* \mathbf{L}^{-1} \mathbf{D}^{-1/2} \mathbf{r} \\ \text{Im } \text{diag}(\mathbf{d})^{-2*} \mathbf{P}^* \mathbf{L}^{-1} \mathbf{D}^{-1/2} \mathbf{r} \end{bmatrix}$;
- 12 $[\underline{\mathbf{L}}]_{:,2k} \leftarrow \underline{\mathbf{Q}}\underline{\mathbf{R}}^{+\top} \begin{bmatrix} \text{Re } \text{diag}(\boldsymbol{\mu}) \text{diag}(\mathbf{d})^{-2*} \mathbf{P}^* \mathbf{L}^{-1} \mathbf{D}^{-1/2} \mathbf{r} \\ \text{Im } \text{diag}(\boldsymbol{\mu}) \text{diag}(\mathbf{d})^{-2*} \mathbf{P}^* \mathbf{L}^{-1} \mathbf{D}^{-1/2} \mathbf{r} \end{bmatrix}$;
- 13 **if** r is odd **then**
- 14 $[\underline{\mathbf{K}}]_{:,r} \leftarrow [\mathbf{I} - \underline{\mathbf{Q}}\underline{\mathbf{Q}}^\top] \begin{bmatrix} \text{Re } \mathbf{D}^{-1/2} \mathbf{L}^{-*} \mathbf{P} \text{diag}(\boldsymbol{\mu} + b_r)^{-2} a_r \\ \text{Im } \mathbf{D}^{-1/2} \mathbf{L}^{-*} \mathbf{P} \text{diag}(\boldsymbol{\mu} + b_r)^{-2} a_r \end{bmatrix}$;
- 15 $[\underline{\mathbf{L}}]_{:,r} \leftarrow \underline{\mathbf{Q}}\underline{\mathbf{R}}^{+\top} \begin{bmatrix} \text{Re } \text{diag}(\boldsymbol{\mu} + b_r)^{-2*} \mathbf{P}^* \mathbf{L}^{-1} \mathbf{D}^{-1/2} \mathbf{r} \\ \text{Im } \text{diag}(\boldsymbol{\mu} + b_r)^{-2*} \mathbf{P}^* \mathbf{L}^{-1} \mathbf{D}^{-1/2} \mathbf{r} \end{bmatrix}$;
- 16 $\mathbf{J} \leftarrow \underline{\mathbf{K}} + \underline{\mathbf{L}}$;

6.3. Optimization. There are many algorithms for nonlinear least squares problems. Here we use Branch, Coleman, and Li’s trust region algorithm [15] as implemented in SciPy’s `least_squares` [32] due to its ability to enforce box constraints. This uses the residual and Jacobian of (6.3), which we compute using Algorithm 6.1.

6.4. Initialization. The rational approximation problem often has many local minimizers with large mismatch. To ensure that we find a good local minimizer with small mismatch, at each step we try two initializations of the optimization algorithm to solve projected problem (6.8), keeping the one with smaller mismatch. One initialization uses the poles of the previous iterate when both are of the same dimension. The other initialization uses the AAA algorithm to construct a degree (r, r) rational approximant ignoring the weighting. As these poles will not in general appear in conjugate pairs—a requirement of $\mathcal{R}_r^+(\mathbb{R})$ —we use the Kuhn-Munkres algorithm to pair these poles with their nearest conjugate-pair, average them, and flip into the left half plane if necessary to find poles of an element of $\mathcal{R}_r^+(\mathbb{R})$.

6.5. Evaluating the Weight Matrix. Cauchy matrices—such as $\mathbf{M}(\boldsymbol{\mu})$ appearing in (6.1)—have a well-deserved reputation for being ill-conditioned. Our application is no exception. As the outer loop converges the entries of $\boldsymbol{\mu}$ become increasingly close and consequently $\mathbf{M}(\boldsymbol{\mu})$ becomes increasingly ill-conditioned. Fortunately the Cauchy matrix structure enables factorizations with high relative accuracy [13, 20]

Algorithm 6.2 Pivoted **LDL*** factorization of $\mathbf{M}(\boldsymbol{\mu})$

Input : $\boldsymbol{\mu} \in \mathbb{C}^n$ determining $[\mathbf{M}(\boldsymbol{\mu})]_{j,k} = (\mu_j + \overline{\mu_k})^{-1}$
Output : Permutation matrix $\mathbf{P} \in \mathbb{R}^{n \times n}$, lower triangular matrix $\mathbf{L} \in \mathbb{C}^{n \times n}$, and diagonal matrix $\mathbf{D} \in \mathbb{R}^{n \times n}$ such that $\mathbf{M}(\boldsymbol{\mu}) = \mathbf{P}\mathbf{L}\mathbf{D}\mathbf{L}^*\mathbf{P}^*$

- 1 $\mathbf{P} = \mathbf{I} \in \mathbb{R}^{n \times n}$;
- 2 $\mathbf{s} \leftarrow (\boldsymbol{\mu} + \overline{\boldsymbol{\mu}})^{-1}$;
- 3 **for** $k = 1, \dots, n$ **do**
- 4 $j \leftarrow \operatorname{argmax}_{j=k, \dots, n} s_j$;
- 5 Permute $\mathbf{P}_{\cdot,k}, \mathbf{P}_{\cdot,j} \leftarrow \mathbf{P}_{\cdot,j}, \mathbf{P}_{\cdot,k}$;
- 6 Permute $\mu_j, \mu_k \leftarrow \mu_k, \mu_j$;
- 7 Permute $s_j, s_k \leftarrow s_k, s_j$;
- 8 $[\mathbf{s}]_{k+1:n} \leftarrow |[\boldsymbol{\mu}]_{k+1:n} - \mu_k|^2 \odot |[\boldsymbol{\mu}]_{k+1:n} + \overline{\mu_k}|^{-2}$
- 9 $\mathbf{g} \leftarrow \mathbf{1} \in \mathbb{C}^n$;
- 10 **for** $k = 1, \dots, n-1$ **do**
- 11 $[\mathbf{D}]_{k,k} \leftarrow \mu_k + \overline{\mu_k}$;
- 12 $[\mathbf{L}]_{k:n,k} \leftarrow [\mathbf{g}]_{k:n} \odot ([\boldsymbol{\mu}]_{k:n} + \overline{\mu_k})^{-1}$;
- 13 $[\mathbf{g}]_{k+1:n} \leftarrow [\mathbf{g}]_{k+1:n} \odot ([\boldsymbol{\mu}]_{k+1:n} - \mu_k) \odot ([\boldsymbol{\mu}]_{k+1:n} + \overline{\mu_k})^{-1}$;
- 14 $[\mathbf{D}]_{n,n} \leftarrow (\mu_n + \overline{\mu_n})^{-1}$;
- 15 $[\mathbf{L}]_{n,n} \leftarrow g_n$;

which we can use to accurately compute the action of $\mathbf{M}(\boldsymbol{\mu})^{-\frac{1}{2}}$. Following Demmel [20, Alg. 3], we compute the Cholesky factorization of $\mathbf{M}(\boldsymbol{\mu})$ using Gaussian elimination with complete pivoting

$$(6.9) \quad \mathbf{M}(\boldsymbol{\mu}) = \mathbf{P}\mathbf{L}\mathbf{D}\mathbf{L}^*\mathbf{P}^*$$

where \mathbf{D} is a diagonal matrix, \mathbf{L} is lower triangular, and \mathbf{P} is a permutation matrix. As $\mathbf{M}(\boldsymbol{\mu})$ is Hermitian, we can preform the necessary pivoting a priori reducing the computational complexity of this decomposition from $\mathcal{O}(n^3)$ to $\mathcal{O}(n^2)$ operations [20, Alg. 4]. Then we evaluate the action of this norm as

$$(6.10) \quad \|P(\boldsymbol{\mu})F\|_{\mathcal{H}_2} = \|\mathbf{M}(\boldsymbol{\mu})^{-\frac{1}{2}}F(\boldsymbol{\mu})\|_2 = \|\mathbf{D}^{-\frac{1}{2}}\mathbf{L}^*\mathbf{P}F(\boldsymbol{\mu})\|_2 \quad \forall F \in \mathcal{H}_2.$$

For completeness, Algorithm 6.2 describes how to compute this high relative accuracy Cholesky factorization where \odot denotes the Hadamard (entry-wise) product.

7. Numerical Experiments. Here we present numerical experiments comparing our Projected \mathcal{H}_2 approach to IRKA, TF-IRKA, and QuadVF. Following the principles of reproducible science, our code implementing these algorithms and generating the figures is available at <https://github.com/jeffrey-hokanson/SYSMOR>.

7.1. Test Problems. Systems with oscillatory behavior prove challenging for model reduction. Our two test problems have significant oscillatory behavior as illustrated by the large number of peaks in their Bode plots in Figures 7.1 and 7.2.

7.1.1. ISS 1R Component. The 1R component of the International Space Station is a standard test problem for model reduction [18, subsec. 2.11] with a sparse state-space representation of dimension 270 with 405 nonzeros. Here we consider the (1, 1) block of this transfer function.

7.1.2. Delay System. Here we slightly modify the delay system from [5, sec. 5]:

$$(7.1) \quad \begin{aligned} H(z) &= \mathbf{c}^\top (z\mathbf{E} - \mathbf{A}_0 - e^{-\tau z} \mathbf{A}_1)^{-1} \mathbf{b} \quad \text{where} \\ \mathbf{E} &:= \frac{2}{\sqrt{\epsilon}} \mathbf{I} + \mathbf{T}, \quad \mathbf{A}_0 := \frac{2+2\rho}{\tau\rho} \left(\mathbf{T} - \frac{2}{\sqrt{\epsilon}} \mathbf{I} \right), \quad \mathbf{A}_1 := \frac{2-2\rho}{\tau\rho} \left(\mathbf{T} - \frac{2}{\sqrt{\epsilon}} \mathbf{I} \right), \end{aligned}$$

$\mathbf{I} \in \mathbb{R}^{n \times n}$ is the identity matrix and $\mathbf{T} \in \mathbb{R}^{n \times n}$ has ones on the first superdiagonal, first subdiagonal, and the $(1,1)$ and (n,n) entries, and is zero otherwise. Here we choose $n = 1000$, $\tau = 1$, $\rho = 0.1$, $\epsilon = 0.01$, pick \mathbf{b} such that its first two entries are one and the remainder zero, and set $\mathbf{c} = \mathbf{b}$.

7.2. Setup. The performance of each algorithm strongly depends on both the choice of the initialization and the termination conditions. Here we describe how we construct comparable conditions for each algorithm.

7.2.1. Initialization. For Projected \mathcal{H}_2 , IRKA, and TF-IRKA each requires an initial set of interpolation points. Following standard practice for IRKA, we choose these interpolation points to be the rightmost r poles of H . For state-space systems, such as the ISS 1R example, these are easily computed from the eigenvalues of \mathbf{A} using an iterative Krylov solver like ARPACK [34]. For the delay example, we computed the poles of H by maximizing $|H(z)|$ starting from pole estimates.

For IRKA and TF-IRKA these r poles provide sufficient data to construct rational interpolants using both transfer function evaluations $H(\mu_j)$ and derivatives $H'(\mu_j)$. However this same initialization yields an underdetermined rational approximation problem in Projected \mathcal{H}_2 as our approach only uses evaluations. Hence, our Projected \mathcal{H}_2 approach constructs lower dimensional reduced order models until sufficient data has been accumulated to yield an overdetermined problem. Note that for the $r = 2$, we do not have sufficient data for an even reduced order model and hence use the four rightmost poles of H in this case only.

QuadVF does not need initial shifts, instead taking fixed samples of H along the imaginary axis. However an initialization is still needed for the vector fitting iteration; here we use the poles from AAA as in our Projected \mathcal{H}_2 approach. We choose scaling parameter $L = 10$ and set the number of quadrature points to approximately equal the number of evaluations of H used by our Projected \mathcal{H}_2 approach at $r = 50$.

7.2.2. Termination Condition. As each algorithm is derived from different principles, each has different natural termination conditions. To provide the same termination condition for each algorithm, we terminate when the difference between successive iterates H_r^ℓ and $H_r^{\ell+1}$ is sufficiently small; namely,

$$(7.2) \quad \|H_r^\ell - H_r^{\ell+1}\|_{\mathcal{H}_2} \leq 10^{-9}.$$

This small tolerance is necessary to avoid premature termination and is easily computed in $\mathcal{O}(r^3)$ operations via (2.4).

7.3. Discussion. As Figures 7.1 and 7.2 illustrate, our Projected \mathcal{H}_2 approach often converges to the similar or a better local minimizer when compared to IRKA, TF-IRKA, and QuadVF. Moreover, our algorithm always uses fewer evaluations of the transfer function than IRKA and TF-IRKA, often by an order of magnitude. This is not an artifact of the tight termination criteria. As the convergence histories in both examples indicate, the Projected \mathcal{H}_2 algorithm converges before both IRKA and TF-IRKA have taken their third step. This improved performance is the result of our

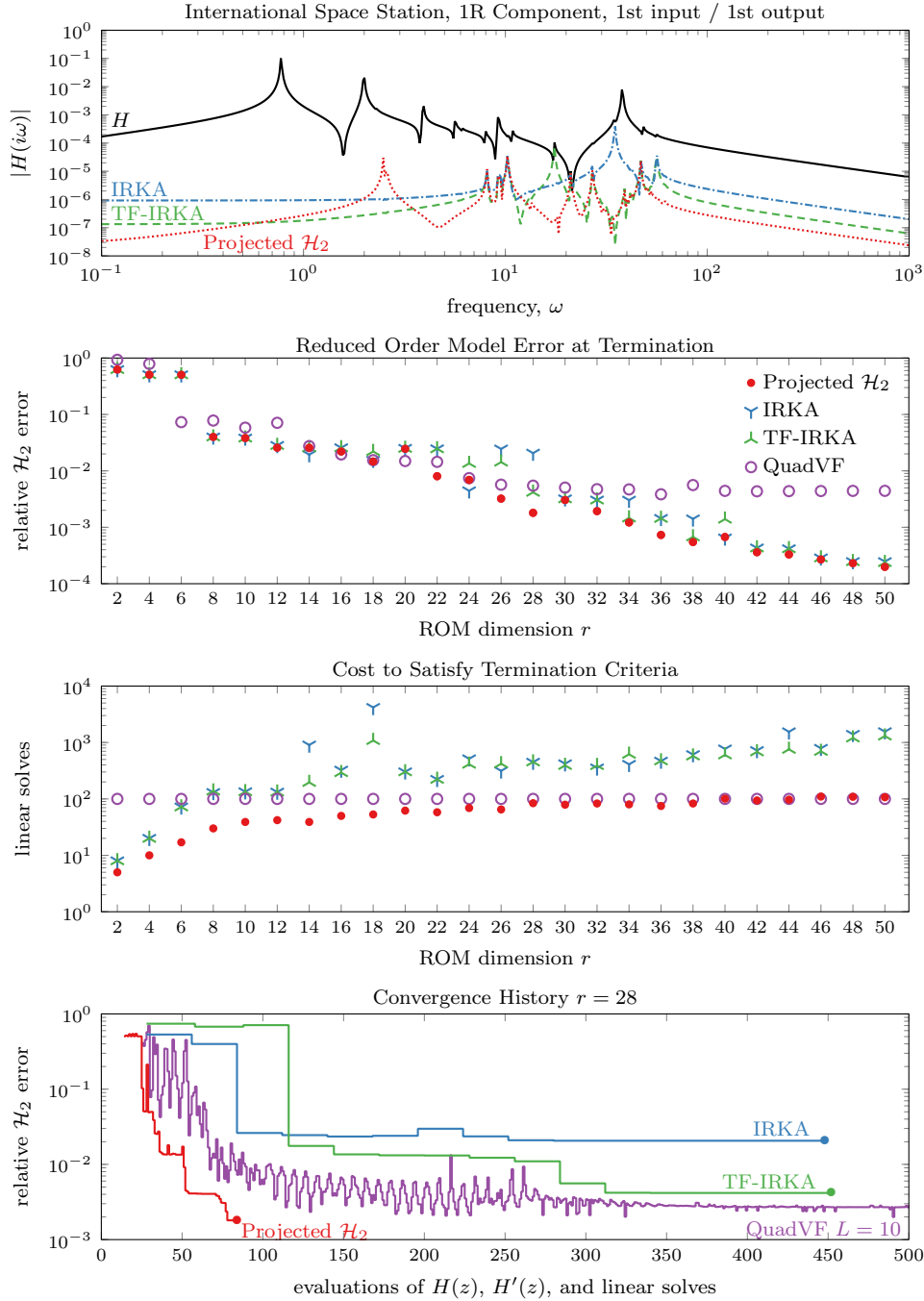


FIG. 7.1. A comparison of model reduction techniques applied the 1R component of the International Space Station described in [18, subsec. 2.11]. The top plot shows the modulus of the transfer function along the imaginary axis, with the broken lines showing the value of the error system $H - H_r$ for different techniques at $r = 28$. The second plot shows the relative \mathcal{H}_2 error for each method for a variety of reduced order model dimensions and the table below shows the number of linear solves, or equivalently, evaluations of $H(z)$ and $H'(z)$ required. The bottom plot shows the convergence history of each of these methods along with a comparison to QuadVF.

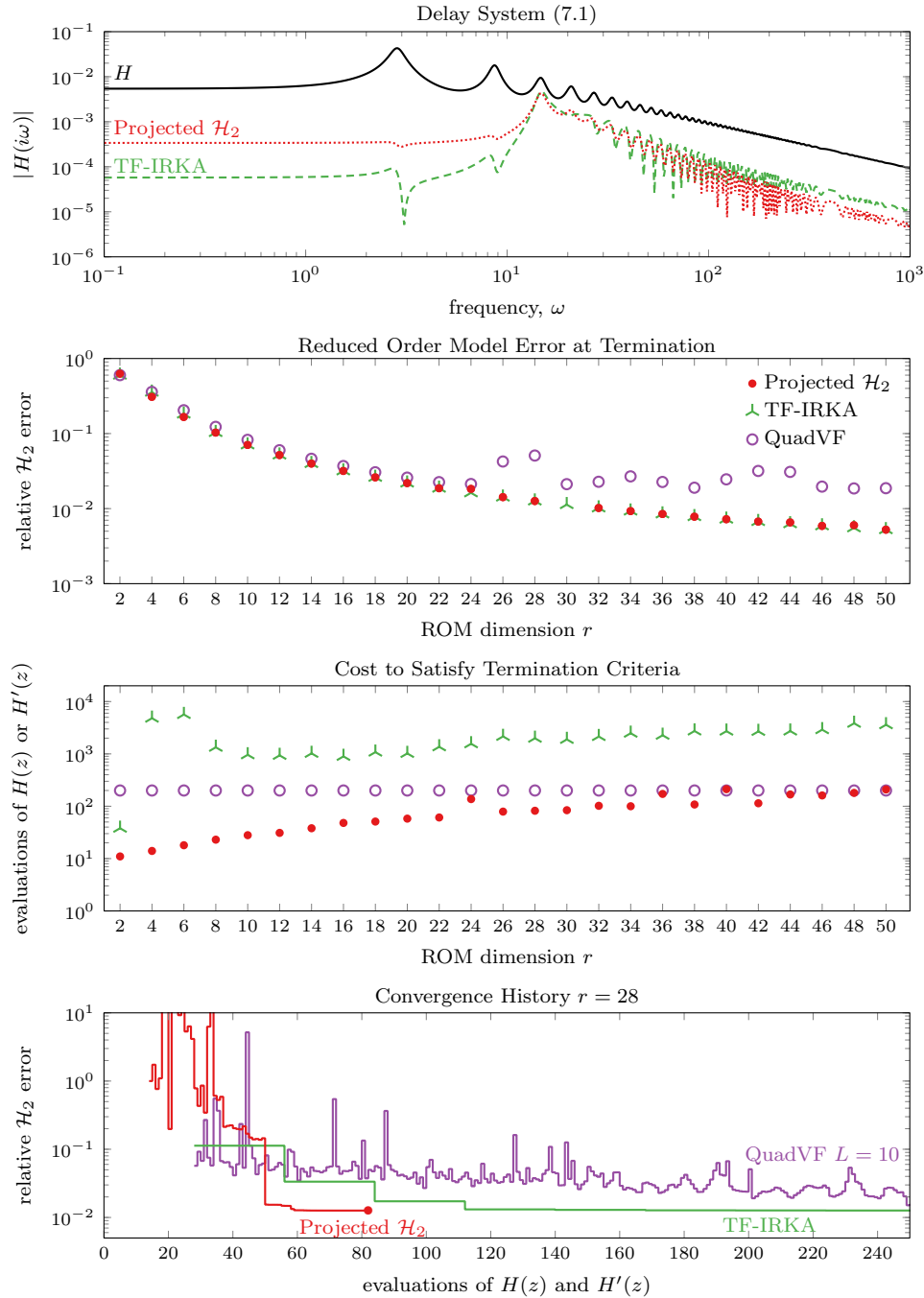


FIG. 7.2. A comparison of model reduction techniques applied the delay system given in (7.1). The top plot shows the modulus of the transfer function along the imaginary axis, with the broken lines showing the value of the error system $H - H_r$ for different techniques at $r = 6$. The second plot shows the relative \mathcal{H}_2 error for each method for a variety of reduced order model dimensions and the table below shows the number of evaluations of $H(z)$ and $H'(z)$ required. The bottom plot shows the convergence history of each of these methods. Here we approximate \mathcal{H}_2 -norm approximately using a Boyd/Clenshaw-Curtis quadrature rule (3.6) with 10^4 quadrature points.

Projected \mathcal{H}_2 approach recycling evaluations of the transfer function between steps whereas IRKA and TF-IRKA must discard previous transfer function evaluations.

These examples also illustrate several properties of the \mathcal{H}_2 model reduction problem. For example, we would expect that $\|H - H_r\|_{\mathcal{H}_2}$ should decrease monotonically with increasing r as $\mathcal{R}_r^+(\mathbb{R}) \subset \mathcal{R}_{r+1}^+(\mathbb{R})$. This is not necessarily true in our experiments as we only recover a local minimizer for each r , not the global minimizer since the \mathcal{H}_2 -model reduction problem is nonconvex.

These examples also illustrate that the error $\|H - \widehat{H}_r^\ell\|_{\mathcal{H}_2}$ does not monotonically decrease with iteration ℓ (note evaluations of H effectively count iterations). For the Projected \mathcal{H}_2 approach this is unsurprising as each \widehat{H}_r^ℓ is locally optimal with respect to the projection $P(\boldsymbol{\mu}^\ell)$ of the \mathcal{H}_2 -norm, not the full \mathcal{H}_2 -norm. In early iterations, the projected norm is a poor approximation of the full norm, leading to inaccurate approximations. This is particularly evident in the delay example.

Finally, we note that our Projected \mathcal{H}_2 approach can fail. In the delay example at $r = 30$, our algorithm terminates with a reduced order model with spurious poles and hence has an exceptionally large mismatch. This illustrates that while the heuristic for removing spurious poles often succeeds, it is not foolproof.

8. Conclusion. We have developed the *Projected \mathcal{H}_2* approach for \mathcal{H}_2 -optimal model reduction problem by applying the projected nonlinear least squares framework to this problem. This allows the \mathcal{H}_2 problem to be converted into a sequence of finite-dimensional rational approximation problems. Although solving these rational approximation problems is more challenging and computationally expensive than constructing rational interpolants as in IRKA and TF-IRKA, this cost is justified by requiring far fewer expensive evaluations of the full order model.

Appendix A. We now provide the proofs for Theorem 4.2 and Theorem 5.1.

A.1. Proof of Theorem 4.2. We begin by rewriting the sine of the subspace angle in terms of the unitary basis operator $B_{\mathcal{T}(\boldsymbol{\lambda})}$ using [12, eq. (13)]

$$(A.1) \quad \begin{aligned} \sin \phi_{\max}(\mathcal{T}(\boldsymbol{\lambda}), \mathcal{V}(\boldsymbol{\mu})) &= \|(I - P(\boldsymbol{\mu}))B_{\mathcal{T}(\boldsymbol{\lambda})}B_{\mathcal{T}(\boldsymbol{\lambda})}^*\|_{\mathcal{H}_2} \\ &= \max_{\mathbf{y} \in \mathbb{C}^{2r}, \|\mathbf{y}\|_2=1} \|(I - P(\boldsymbol{\mu}))B_{\mathcal{T}(\boldsymbol{\lambda})}\mathbf{y}\|_{\mathcal{H}_2}. \end{aligned}$$

As $I - P(\boldsymbol{\mu})$ is an orthogonal projector onto the complement of $\mathcal{V}(\boldsymbol{\mu})$, its projection satisfies the closest point property. This permits an equivalent restatement as

$$(A.2) \quad \sin \phi_{\max}(\mathcal{T}(\boldsymbol{\lambda}), \mathcal{V}(\boldsymbol{\mu})) = \max_{\mathbf{y} \in \mathbb{C}^{2r}, \|\mathbf{y}\|_2=1} \min_{\mathbf{x} \in \mathbb{C}^n} \|B_{\mathcal{T}(\boldsymbol{\lambda})}\mathbf{y} + V(\boldsymbol{\mu})\mathbf{x}\|_{\mathcal{H}_2}.$$

Writing this in terms of the non-orthogonal basis vectors for $\mathcal{T}(\boldsymbol{\lambda})$ and $\mathcal{V}(\boldsymbol{\mu})$,

$$(A.3) \quad \sin \phi_{\max}(\mathcal{T}(\boldsymbol{\lambda}), \mathcal{V}(\boldsymbol{\mu})) = \max_{\substack{\mathbf{z} \in \mathbb{C}^{2r} \\ \mathbf{z} \neq 0}} \min_{\mathbf{x} \in \mathbb{C}^n} \frac{\| [V(-\bar{\boldsymbol{\lambda}}) \quad V'(-\bar{\boldsymbol{\lambda}})] \mathbf{z} + V(\boldsymbol{\mu})\mathbf{x} \|_{\mathcal{H}_2}}{\|\widehat{\mathbf{M}}(\boldsymbol{\lambda})\mathbf{z}\|_2}.$$

We now bound the numerator by making a non-optimal choice of \mathbf{x} . Denoting the entries of \mathbf{x} associated with $\mu_{k,i}$ as $x_{k,i}$ and setting the remainder to zero, we have

$$(A.4) \quad \begin{aligned} &\min_{\mathbf{x} \in \mathbb{C}^n} \| [V(-\bar{\boldsymbol{\lambda}}) \quad V'(-\bar{\boldsymbol{\lambda}})] \mathbf{z} - V(\boldsymbol{\mu})\mathbf{x} \|_{\mathcal{H}_2} \\ &\leq \min_{\substack{\{x_{k,1}\}_{k=1}^m \subset \mathbb{C} \\ \{x_{k,2}\}_{k=1}^m \subset \mathbb{C} \\ \{x_{k,3}\}_{k=1}^m \subset \mathbb{C}}} \left\| \sum_{k=1}^m v[-\bar{\lambda}_k]z_{k,1} + v[-\bar{\lambda}_k]'z_{k,2} + v[\mu_{k,1}]x_{k,1} + v[\mu_{k,2}]x_{k,2} + v[\mu_{k,3}]x_{k,3} \right\|_{\mathcal{H}_2}. \end{aligned}$$

Applying the triangle inequality to groups of $v[-\bar{\lambda}_k]$ with $v[\mu_{k,1}]$ and $v'[-\bar{\lambda}_k]$ with $v[\mu_{k,2}]$ and $v[\mu_{k,3}]$ provides the bound

$$(A.5) \quad \min_{\mathbf{x} \in \mathbb{C}^n} \left\| [V(-\bar{\lambda}) \quad V'(-\bar{\lambda})] \mathbf{z} - V(\boldsymbol{\mu}) \mathbf{x} \right\|_{\mathcal{H}_2} \leq \sum_{k=1}^m \min_{x_{k,1} \in \mathbb{C}} \|v[-\bar{\lambda}_k] z_{k,1} + v[\mu_{k,1}] x_{k,1}\|_{\mathcal{H}_2} + \min_{\substack{x_{k,2} \in \mathbb{C} \\ x_{k,3} \in \mathbb{C}}} \|v[-\bar{\lambda}_k]' z_{k,2} + v[\mu_{k,2}] x_{k,2} + v[\mu_{k,3}] x_{k,3}\|_{\mathcal{H}_2}$$

where in each term, the minimization has been pulled inside the sum as each of $x_{k,1}$ and $x_{k,2}, x_{k,3}$ appear in only one term.

Now we bound each of these minimizations in (A.5) separately. To simplify notation, we omit the subscripts in the next paragraph. For the first term of (A.5)

$$(A.6) \quad \|v[-\bar{\lambda}] z_1 + v[\mu_1] x_1\|_{\mathcal{H}_2}^2 = \frac{x_1 \bar{x}_1}{\mu_1 + \bar{\mu}_1} + \frac{x_1 \bar{z}_1}{\bar{\mu}_1 - \bar{\lambda}} + \frac{\bar{x}_1 z_1}{\mu_1 - \lambda} - \frac{z_1 \bar{z}_1}{\bar{\lambda} + \lambda}.$$

As $(\mu_1 + \bar{\mu}_1)^{-1}$ is positive, this is convex in x_1 . Thus a value of x_1 satisfying the first order necessary conditions is also the global minimizer. Using Wirtinger calculus [40, App. A], the first order necessary conditions for minimization over x_1 are

$$(A.7) \quad \begin{cases} 0 = x_1(\mu_1 + \bar{\mu}_1)^{-1} + z_1(\mu_1 - \lambda)^{-1} \\ 0 = \bar{x}_1(\mu_1 + \bar{\mu}_1)^{-1} + \bar{z}_1(\bar{\mu}_1 - \bar{\lambda})^{-1} \end{cases} \implies x_1 = -z_1 \frac{\mu_1 + \bar{\mu}_1}{\mu_1 - \lambda}.$$

Substituting this value of x_1 provides the bound

$$(A.8) \quad \min_{x_1 \in \mathbb{C}} \|v[-\bar{\lambda}] z_1 + v[\mu_1] x_1\|_{\mathcal{H}_2}^2 = |z_1|^2 \frac{|\mu_1 + \bar{\lambda}|^2}{2|\mu_1 - \lambda|^2 \operatorname{Re}[-\bar{\lambda}]} \leq |z_1|^2 C_1^2 \epsilon^2.$$

where $C_1 > 0$ is a constant independent of ϵ . For the second term we first insert the additive identity $0 = v'[\mu_2] - v'[\mu_2]$ and apply the triangle inequality to simplify the resulting arithmetic:

$$(A.9) \quad \|v[-\bar{\lambda}]' z_2 + v[\mu_2] x_2 + v[\mu_3] x_3\|_{\mathcal{H}_2} = |z_2| \|v[-\bar{\lambda}]' - v[\mu_2]'\|_{\mathcal{H}_2} + \|v[\mu_2]' z_2 + v[\mu_2] x_2 + v[\mu_3] x_3\|_{\mathcal{H}_2}.$$

After some simplification, the first term above has the bound

$$(A.10) \quad \|v[-\bar{\lambda}]' - v[\mu_2]'\|_{\mathcal{H}_2}^2 = \frac{2}{(-\bar{\lambda} - \lambda)^3} - \frac{2}{(-\bar{\lambda} + \bar{\mu}_2)^3} - \frac{2}{(\mu_2 - \lambda)^3} + \frac{2}{(\mu_2 + \bar{\mu}_2)^3} = 2 \frac{|\mu_2 + \bar{\lambda}|^2 p(\mu_2, \lambda, \bar{\mu}_2, \bar{\lambda})}{|\lambda - \mu_2|^6 \operatorname{Re}[2\mu_2]^3 \operatorname{Re}[-2\lambda]^3} \leq C_2^2 \epsilon^2$$

where $p(\mu_2, \lambda, \bar{\mu}_2, \bar{\lambda})$ is a degree-7 polynomial and $C_2 > 0$ is independent of ϵ . To bound the second part of (A.9), first note

$$(A.11) \quad \|v[\mu_2] x_2 + v[\mu_3] x_3 + v[\mu_2]' z_2\|_{\mathcal{H}_2}^2 = \begin{bmatrix} x_2 \\ x_3 \\ z_2 \end{bmatrix}^* \begin{bmatrix} (\mu_2 + \bar{\mu}_2)^{-1} & (\mu_2 + \bar{\mu}_3)^{-1} & -(\mu_2 + \bar{\mu}_2)^{-2} \\ (\mu_3 + \bar{\mu}_2)^{-1} & (\mu_3 + \bar{\mu}_3)^{-1} & -(\mu_3 + \bar{\mu}_2)^{-2} \\ -(\mu_2 + \bar{\mu}_2)^{-2} & -(\mu_2 + \bar{\mu}_3)^{-2} & 2(\bar{\mu}_2 + \mu_2)^{-3} \end{bmatrix} \begin{bmatrix} x_2 \\ x_3 \\ z_2 \end{bmatrix}.$$

As the upper left 2×2 block is positive definite, minimizing this quantity with respect to $\begin{bmatrix} x_2 \\ x_3 \end{bmatrix}$ for a fixed z_2 is strictly convex and hence the point satisfying the first order necessary conditions is also the global minimizer. Using Wirtinger calculus, these conditions require

$$(A.12) \quad \begin{bmatrix} x_2 \\ x_3 \end{bmatrix}^* \begin{bmatrix} (\mu_2 + \bar{\mu}_2)^{-1} & (\mu_2 + \bar{\mu}_3)^{-1} \\ (\mu_3 + \bar{\mu}_2)^{-1} & (\mu_3 + \bar{\mu}_3)^{-1} \end{bmatrix} + \bar{z}_2 \begin{bmatrix} -(\mu_2 + \bar{\mu}_2)^{-2} \\ -(\mu_3 + \bar{\mu}_2)^{-2} \end{bmatrix}^* = \mathbf{0},$$

$$(A.13) \quad \begin{bmatrix} x_2 \\ x_3 \end{bmatrix}^\top \begin{bmatrix} (\mu_2 + \bar{\mu}_2)^{-1} & (\mu_2 + \bar{\mu}_3)^{-1} \\ (\mu_3 + \bar{\mu}_2)^{-1} & (\mu_3 + \bar{\mu}_3)^{-1} \end{bmatrix} + z_2 \begin{bmatrix} -(\mu_2 + \bar{\mu}_2)^{-2} \\ -(\mu_3 + \bar{\mu}_2)^{-2} \end{bmatrix}^\top = \mathbf{0}.$$

Hence we conclude

$$(A.14) \quad \begin{bmatrix} x_2 \\ x_3 \end{bmatrix} = z_2 \begin{bmatrix} (\mu_2 + \bar{\mu}_2)^{-1} & (\mu_2 + \bar{\mu}_3)^{-1} \\ (\mu_3 + \bar{\mu}_2)^{-1} & (\mu_3 + \bar{\mu}_3)^{-1} \end{bmatrix}^{-1} \begin{bmatrix} (\mu_2 + \bar{\mu}_2)^{-2} \\ (\mu_3 + \bar{\mu}_2)^{-2} \end{bmatrix}^*.$$

Making this substitution and simplifying, we bound this quantity by

$$(A.15) \quad \min_{x_2, x_3 \in \mathbb{C}} \|v[-\bar{\lambda}]' z_2 + v[\mu_2] x_2 + v[\mu_3] x_3\|_{\mathcal{H}_2}^2 = \frac{|z_2|^2 |\mu_2 - \mu_3|^2}{\operatorname{Re}[2\mu_2]^3 |\mu_2 + \bar{\mu}_3|^2} \leq C_3^2 |z_2|^2 \epsilon^2$$

where $C_3 > 0$ is independent of ϵ .

Finally we combine these bounds to obtain the desired bound on the subspace angle. Returning to (A.5) and applying the bounds from (A.8), (A.10), and (A.15)

$$(A.16) \quad \min_{\mathbf{x} \in \mathbb{C}^n} \|[V(-\bar{\lambda}) \ V'(-\bar{\lambda})] \mathbf{z} - V(\boldsymbol{\mu}) \mathbf{x}\|_{\mathcal{H}_2} \leq \epsilon \sum_{k=1}^m C_{k,1} |z_{k,1}| + \sqrt{C_{k,2}^2 + C_{k,3}^2} |z_{k,2}|.$$

Then invoking the lower bound $\|\widehat{\mathbf{M}}(\boldsymbol{\lambda}) \mathbf{z}\|_2 \geq \sigma_{\min}(\widehat{\mathbf{M}}(\boldsymbol{\lambda})) \|\mathbf{z}\|_\infty$ and that $\widehat{\mathbf{M}}(\boldsymbol{\lambda})$ is positive definite and independent of ϵ , we can bound the subspace angle in (A.3) by

$$(A.17) \quad \sin \phi_{\max}(\mathcal{T}(\boldsymbol{\lambda}), \mathcal{V}(\boldsymbol{\mu})) \leq \epsilon \left[\sigma_{\min}^{-1}(\widehat{\mathbf{M}}(\boldsymbol{\lambda})) \sum_{k=1}^m C_{k,1} + \sqrt{C_{k,2}^2 + C_{k,3}^2} \right].$$

A.2. Proof of Theorem 5.1. We begin by establishing a basic subspace angle result analogous to those in the previous proof.

LEMMA A.1. *If $\lambda_1, \lambda_2 \in \mathbb{C}_-$, then*

$$(A.18) \quad \sin \phi_{\max}(\mathcal{T}(\lambda_1), \mathcal{T}(\lambda_2)) \leq C |\lambda_1 - \lambda_2|.$$

Proof. Following the proof of Theorem 4.2 in equations (A.1) and (A.3) we can write this subspace angle as

$$(A.19) \quad \sin \phi_{\max}(\mathcal{T}(\lambda_1), \mathcal{T}(\lambda_2)) \\ = \max_{z \in \mathbb{C}^2} \min_{\substack{\mathbf{x} \in \mathbb{C}^2 \\ \mathbf{z} \neq \mathbf{0}}} \frac{\|v[-\bar{\lambda}_1] z_1 + v[-\bar{\lambda}_1]' z_2 + v[-\bar{\lambda}_2] x_1 + v[-\bar{\lambda}_2]' x_2\|_{\mathcal{H}_2}}{\|v[-\bar{\lambda}_1] z_1 + v[-\bar{\lambda}_1]' z_2\|_{\mathcal{H}_2}}.$$

Writing out the numerator explicitly and splitting into 2×2 blocks,

$$\begin{aligned}
\text{(A.20)} \quad & \|v[-\bar{\lambda}_1]z_1 + v[-\bar{\lambda}_1]'z_2 + v[-\bar{\lambda}_2]x_1 + v[-\bar{\lambda}_2]'x_2\|_{\mathcal{H}_2}^2 \\
&= \begin{bmatrix} z_1 \\ z_2 \\ x_1 \\ x_2 \end{bmatrix}^* \begin{bmatrix} (-\bar{\lambda}_1 - \lambda_1)^{-1} & -(-\bar{\lambda}_1 - \lambda_1)^{-2} & (-\bar{\lambda}_1 - \lambda_2)^{-1} & -(-\bar{\lambda}_1 - \lambda_2)^{-2} \\ -(-\bar{\lambda}_1 - \lambda_1)^{-2} & 2(-\bar{\lambda}_1 - \lambda_1)^{-3} & -(\bar{\lambda}_1 - \lambda_2)^{-2} & 2(-\bar{\lambda}_1 - \lambda_2)^{-3} \\ (-\bar{\lambda}_2 - \lambda_1)^{-1} & -(-\bar{\lambda}_2 - \lambda_1)^{-2} & (-\bar{\lambda}_2 - \lambda_2)^{-1} & -(-\bar{\lambda}_2 - \lambda_2)^{-2} \\ -(-\bar{\lambda}_2 - \lambda_1)^{-2} & 2(-\bar{\lambda}_2 - \lambda_1)^{-3} & -(\bar{\lambda}_2 - \lambda_2)^{-2} & 2(-\bar{\lambda}_2 - \lambda_2)^{-3} \end{bmatrix} \begin{bmatrix} z_1 \\ z_2 \\ x_1 \\ x_2 \end{bmatrix} \\
&= \begin{bmatrix} \mathbf{z} \\ \mathbf{x} \end{bmatrix}^* \begin{bmatrix} \widehat{\mathbf{M}}_1 & \mathbf{C} \\ \mathbf{C}^* & \widehat{\mathbf{M}}_2 \end{bmatrix} \begin{bmatrix} \mathbf{z} \\ \mathbf{x} \end{bmatrix} = \mathbf{z}^* \widehat{\mathbf{M}}_1 \mathbf{z} + \mathbf{x}^* \mathbf{C}^* \mathbf{z} + \mathbf{z}^* \mathbf{C} \mathbf{x} + \mathbf{x}^* \widehat{\mathbf{M}}_2 \mathbf{x}.
\end{aligned}$$

Minimizing over \mathbf{x} holding \mathbf{z} fixed is a strictly convex problem with a unique global minimizer. From Wirtinger calculus this minimizer is $\mathbf{x} = -\widehat{\mathbf{M}}_2^{-1} \mathbf{C}^* \mathbf{z}$. Substituting this value yields the minimum

$$\text{(A.21)} \quad \min_{\mathbf{x} \in \mathbb{C}^2} \|v[-\bar{\lambda}_1]z_1 + v[-\bar{\lambda}_1]'z_2 + v[-\bar{\lambda}_2]x_1 + v[-\bar{\lambda}_2]'x_2\|_{\mathcal{H}_2}^2 = \mathbf{z}^* [\widehat{\mathbf{M}}_1 - \mathbf{C} \widehat{\mathbf{M}}_2^{-1} \mathbf{C}^*] \mathbf{z}.$$

The entries of this interior matrix are all of order $|\lambda_1 - \lambda_2|$:

$$\text{(A.22)} \quad [\widehat{\mathbf{M}}_1 - \mathbf{C} \widehat{\mathbf{M}}_2^{-1} \mathbf{C}^*]_{1,1} = \frac{|\lambda_1 - \lambda_2|^2 p_1(\lambda_1, \lambda_2, \bar{\lambda}_1, \bar{\lambda}_2)}{3(\lambda_1 + \bar{\lambda}_1)^2 |\lambda_1 + \bar{\lambda}_2|^4};$$

$$\text{(A.23)} \quad [\widehat{\mathbf{M}}_1 - \mathbf{C} \widehat{\mathbf{M}}_2^{-1} \mathbf{C}^*]_{1,2} = \frac{|\lambda_1 - \lambda_2|^2 p_2(\lambda_1, \lambda_2, \bar{\lambda}_1, \bar{\lambda}_2)}{(\lambda_1 + \bar{\lambda}_1)^2 (\lambda_1 + \bar{\lambda}_2)^3 (\bar{\lambda}_1 + \lambda_2)^2};$$

$$\text{(A.24)} \quad [\widehat{\mathbf{M}}_1 - \mathbf{C} \widehat{\mathbf{M}}_2^{-1} \mathbf{C}^*]_{2,2} = \frac{|\lambda_1 - \lambda_2|^2 p_3(\lambda_1, \lambda_2, \bar{\lambda}_1, \bar{\lambda}_2)}{3(\lambda_1 + \bar{\lambda}_1)^3 |\lambda_1 + \bar{\lambda}_2|^6};$$

where p_1 , p_2 , and p_3 are all polynomials. Then as $\widehat{\mathbf{M}}_1$ is positive definite, the maximization over \mathbf{z} is bounded above by some constant C multiplied by $|\lambda_1 - \lambda_2|$. \square

Proof of Theorem 5.1. Our goal will be to show that \widehat{H}_r satisfies the first order optimality conditions (4.22): namely $\|Q(\widehat{\boldsymbol{\lambda}})[H - \widehat{H}_r]\|_{\mathcal{H}_2}$ is zero where $\widehat{\boldsymbol{\lambda}}$ denotes the poles of \widehat{H}_r . To begin, we insert the additive identity $0 = \widehat{H}_r^\ell - \widehat{H}_r^\ell$ and apply the triangle inequality

$$\text{(A.25)} \quad \|Q(\widehat{\boldsymbol{\lambda}})[H - \widehat{H}_r]\|_{\mathcal{H}_2} \leq \|Q(\widehat{\boldsymbol{\lambda}})[H - \widehat{H}_r^\ell]\|_{\mathcal{H}_2} + \|Q(\widehat{\boldsymbol{\lambda}})[\widehat{H}_r - \widehat{H}_r^\ell]\|_{\mathcal{H}_2}$$

$$\text{(A.26)} \quad \leq \|Q(\widehat{\boldsymbol{\lambda}})[H - \widehat{H}_r^\ell]\|_{\mathcal{H}_2} + \|Q(\widehat{\boldsymbol{\lambda}})\|_{\mathcal{H}_2} \|\widehat{H}_r - \widehat{H}_r^\ell\|_{\mathcal{H}_2}$$

As $Q(\widehat{\boldsymbol{\lambda}})$ is a projector, $\|Q(\widehat{\boldsymbol{\lambda}})\|_{\mathcal{H}_2} = 1$. Next we insert the multiplicative identity $I = P(\boldsymbol{\mu}^\ell) + (I - P(\boldsymbol{\mu}^\ell))$ and again apply the triangle inequality

$$\begin{aligned}
\text{(A.27)} \quad & \|Q(\widehat{\boldsymbol{\lambda}})[H - \widehat{H}_r]\|_{\mathcal{H}_2} \leq \|Q(\widehat{\boldsymbol{\lambda}})P(\boldsymbol{\mu}^\ell)[H - \widehat{H}_r^\ell]\|_{\mathcal{H}_2} \\
& \quad + \|Q(\widehat{\boldsymbol{\lambda}})[I - P(\boldsymbol{\mu}^\ell)][H - \widehat{H}_r^\ell]\|_{\mathcal{H}_2} + \|\widehat{H}_r - \widehat{H}_r^\ell\|_{\mathcal{H}_2}.
\end{aligned}$$

We split the first term by inserting the multiplicative identity $I = Q(\widehat{\boldsymbol{\lambda}}^\ell) + (I - Q(\widehat{\boldsymbol{\lambda}}^\ell))$ where $\widehat{\boldsymbol{\lambda}}^\ell$ denotes the poles of \widehat{H}_r^ℓ and again applying the triangle inequality

$$\begin{aligned}
\text{(A.28)} \quad & \|Q(\widehat{\boldsymbol{\lambda}})[H - \widehat{H}_r]\|_{\mathcal{H}_2} \leq \|Q(\widehat{\boldsymbol{\lambda}})Q(\widehat{\boldsymbol{\lambda}}^\ell)P(\boldsymbol{\mu}^\ell)[H - \widehat{H}_r^\ell]\|_{\mathcal{H}_2} \\
& + \|Q(\widehat{\boldsymbol{\lambda}})[I - Q(\widehat{\boldsymbol{\lambda}}^\ell)]P(\boldsymbol{\mu}^\ell)[H - \widehat{H}_r^\ell]\|_{\mathcal{H}_2} + \|Q(\widehat{\boldsymbol{\lambda}})[I - P(\boldsymbol{\mu}^\ell)][H - \widehat{H}_r^\ell]\|_{\mathcal{H}_2} + \|\widehat{H}_r - \widehat{H}_r^\ell\|_{\mathcal{H}_2}.
\end{aligned}$$

Since \widehat{H}_r^ℓ satisfies the first order optimality conditions then $Q(\widehat{\lambda}^\ell)P(\mu^\ell)[H - \widehat{H}_r^\ell] = 0$, cf. (4.23), and hence the first term vanishes. For the remaining terms we use the fact the induced \mathcal{H}_2 -norm is submultiplicative

$$(A.29) \quad \begin{aligned} \|Q(\widehat{\lambda})[H - \widehat{H}_r]\|_{\mathcal{H}_2} &\leq \|Q(\widehat{\lambda})[I - Q(\widehat{\lambda}^\ell)]\|_{\mathcal{H}_2} \| [H - \widehat{H}_r^\ell] \|_{\mathcal{H}_2} \\ &\quad + \|Q(\widehat{\lambda})[I - P(\mu^\ell)]\|_{\mathcal{H}_2} \| [H - \widehat{H}_r^\ell] \|_{\mathcal{H}_2} + \| \widehat{H}_r - \widehat{H}_r^\ell \|_{\mathcal{H}_2}. \end{aligned}$$

We will now show that for any $\epsilon > 0$, there is an $N > 0$ such that for all $\ell > N$ each term above is bounded by an order ϵ term and thus $\|Q(\widehat{\lambda})[H - \widehat{H}_r]\|_{\mathcal{H}_2}$ is zero.

For the first term in (A.29), we first establish $\widehat{\lambda}^\ell \rightarrow \widehat{\lambda}$ as $\ell \rightarrow \infty$ under the proper ordering. As we assume $\widehat{H}_r \in \mathcal{R}_r^+(\mathbb{C})$ has r distinct poles, we can write \widehat{H}_r in pole-residue form

$$(A.30) \quad \widehat{H}_r(z) = \sum_{j=1}^r \widehat{\rho}_j (z - \widehat{\lambda}_j)^{-1} \quad \text{where} \quad |\rho_j| > 0$$

as otherwise \widehat{H}_r would have fewer than r poles. As rational functions with higher order poles are nowhere dense in $\mathcal{R}_r^+(\mathbb{C})$ [22, p. 2739] and $\widehat{H}_r^\ell \rightarrow \widehat{H}_r$ there is some $N_1 > 0$ for which all \widehat{H}_r^ℓ with $\ell > N_1$ has no higher order poles and thus has a pole-residue form

$$(A.31) \quad \widehat{H}_r^\ell(z) = \sum_{j=1}^r \widehat{\rho}_j^\ell (z - \widehat{\lambda}_j^\ell)^{-1} \quad \forall \ell > N_1.$$

As the pole-residue form is unique up to permutations, then as $\widehat{H}_r^\ell \rightarrow \widehat{H}_r$, $\widehat{\lambda}_j^\ell \rightarrow \widehat{\lambda}_j$. Next we bound $\|Q(\widehat{\lambda})[I - Q(\widehat{\lambda}^\ell)]\|_{\mathcal{H}_2}$. We begin by inserting the multiplicative identity $Q(\widehat{\lambda}_j) + [I - Q(\widehat{\lambda}_j)]$ and applying the triangle inequality

$$(A.32) \quad \begin{aligned} \|Q(\widehat{\lambda})[I - Q(\widehat{\lambda}^\ell)]\|_{\mathcal{H}_2} &\leq \sum_{j=1}^r \|Q(\widehat{\lambda})Q(\widehat{\lambda}_j)[I - Q(\widehat{\lambda}^\ell)]\|_{\mathcal{H}_2} + \|Q(\widehat{\lambda})[I - Q(\widehat{\lambda}_j)][I - Q(\widehat{\lambda}^\ell)]\|_{\mathcal{H}_2}. \end{aligned}$$

As $\text{Range } Q(\widehat{\lambda}_j) \subset \text{Range } Q(\widehat{\lambda})$, $Q(\widehat{\lambda})[I - Q(\widehat{\lambda}_j)] = 0$ and the second term vanishes. Then pulling out $Q(\widehat{\lambda})$ using the submultiplicative property and noting $\|Q(\widehat{\lambda})\|_{\mathcal{H}_2} = 1$,

$$(A.33) \quad \|Q(\widehat{\lambda})[I - Q(\widehat{\lambda}^\ell)]\|_{\mathcal{H}_2} \leq \sum_{j=1}^r \|Q(\widehat{\lambda})\|_{\mathcal{H}_2} \|Q(\widehat{\lambda}_j)[I - Q(\widehat{\lambda}^\ell)]\|_{\mathcal{H}_2}$$

$$(A.34) \quad \leq \sum_{j=1}^r \|Q(\widehat{\lambda}_j)[I - Q(\widehat{\lambda}^\ell)]\|_{\mathcal{H}_2}.$$

A similar approach is used on the $[I - Q(\widehat{\lambda}^\ell)]$ term: inserting the multiplicative identity $Q(\widehat{\lambda}_j^\ell) + (I - Q(\widehat{\lambda}_j^\ell))$ and applying the triangle inequality

$$(A.35) \quad \begin{aligned} \|Q(\widehat{\lambda})[I - Q(\widehat{\lambda}^\ell)]\|_{\mathcal{H}_2} &\leq \sum_{j=1}^r \|Q(\widehat{\lambda}_j)Q(\widehat{\lambda}_j^\ell)[I - Q(\widehat{\lambda}^\ell)]\|_{\mathcal{H}_2} \\ &\quad + \|Q(\widehat{\lambda}_j)[I - Q(\widehat{\lambda}_j^\ell)][I - Q(\widehat{\lambda}^\ell)]\|_{\mathcal{H}_2}. \end{aligned}$$

As $\text{Range } Q(\lambda_j^\ell) \subset \text{Range } Q(\widehat{\lambda}^\ell)$, consequently $Q(\lambda_j^\ell)[I - Q(\widehat{\lambda}^\ell)] = 0$ and thus the first term is zero. Then extracting $I - Q(\widehat{\lambda}^\ell)$ via the submultiplicative property and noting this is also an orthogonal projector, we have

$$(A.36) \quad \|Q(\widehat{\lambda})[I - Q(\widehat{\lambda}^\ell)]\|_{\mathcal{H}_2} \leq \sum_{j=1}^r \|Q(\widehat{\lambda}_j)[I - Q(\lambda_j^\ell)]\|_{\mathcal{H}_2} \|I - Q(\widehat{\lambda}^\ell)\|_{\mathcal{H}_2}$$

$$(A.37) \quad \leq \sum_{j=1}^r \|Q(\widehat{\lambda}_j)[I - Q(\lambda_j^\ell)]\|_{\mathcal{H}_2}.$$

Invoking Lemma A.1,

$$(A.38) \quad \|Q(\widehat{\lambda})[I - Q(\widehat{\lambda}^\ell)]\|_{\mathcal{H}_2} \leq \sum_{j=1}^r C_j |\widehat{\lambda}_j - \widehat{\lambda}_j^\ell|.$$

Then as $\widehat{\lambda}_j^\ell \rightarrow \widehat{\lambda}_j$, for any $\epsilon > 0$ there is some $N_2 > 0$ such that for all $\ell > N_2$ $|\widehat{\lambda}_j^\ell - \widehat{\lambda}_j| < \epsilon$ and thus the first term in (A.29) is order ϵ

$$(A.39) \quad \|Q(\widehat{\lambda})[I - Q(\widehat{\lambda}^\ell)]\|_{\mathcal{H}_2} \leq \epsilon \sum_{j=1}^r C_j \quad \forall \ell > N_2.$$

For the second term in (A.29), we first bound this quantity in terms of individual $Q(\widehat{\lambda}_j)$ following the same process as in (A.32) and (A.33):

$$(A.40) \quad \|Q(\widehat{\lambda})[I - P(\boldsymbol{\mu}^\ell)]\|_{\mathcal{H}_2} \leq \sum_{j=1}^r \|Q(\widehat{\lambda}_j)[I - P(\boldsymbol{\mu}^\ell)]\|_{\mathcal{H}_2}.$$

We will first show that one of these terms is order ϵ and then show that the remainder must be order ϵ as well. As the sequence of $\{\mu_\star^\ell\}_{\ell=0}^\infty$ is bounded, there is at least one convergent subsequence with accumulation point $\widehat{\mu}$. Since this sequence is constructed from the poles $\widehat{\lambda}^\ell$ of \widehat{H}_r^ℓ , the limit points of $\{\mu_\star^\ell\}_{\ell=0}^\infty$ must be a subset of the limit points of $\{-\widehat{\lambda}^\ell\}_{\ell=0}^\infty$; namely the poles $\widehat{\lambda}$ of \widehat{H}_r . Thus there is some k where $-\widehat{\mu} = \widehat{\lambda}_k$. Then as $\widehat{\mu}$ is an accumulation point, for any $\epsilon > 0$ there is some N_3 such that $\{\mu_\star^\ell\}_{\ell=0}^{N_3} \cap \mathcal{B}_\epsilon(-\widehat{\lambda}_k)$ has at least three elements. Hence by Theorem 4.2,

$$(A.41) \quad \sin \phi_{\max}(\mathcal{T}(\widehat{\lambda}_k), \mathcal{V}(\boldsymbol{\mu}^\ell)) \leq C\epsilon, \quad \text{note } \boldsymbol{\mu}^\ell = [\mu^0 \quad \mu_\star^0 \quad \mu_\star^1 \quad \cdots \quad \mu_\star^{\ell-1}].$$

Hence $\|Q(\widehat{\lambda}_k)[I - P(\boldsymbol{\mu}^\ell)]\|_{\mathcal{H}_2} \rightarrow 0$ as $\ell \rightarrow \infty$. To show the remaining terms of (A.40) are bounded in ϵ , first note that as $\widehat{\mu}$ is an accumulation point there is some $N_4 > N_3$ where $\mu_\star^{N_4} \in \mathcal{B}_\epsilon(\widehat{\mu})$; moreover we can choose this N_4 such that $|\widehat{\lambda}_j - \widehat{\lambda}_j^\ell| \leq \epsilon$ for all $\ell > N_4$. For this value of N_4 , $\lambda_\star^{N_4} = \widehat{\lambda}_k^{N_4}$. Thus we have by construction of $\mu_\star^{N_4}$ in (5.6)

$$(A.42) \quad \sin \phi_{\max}(\mathcal{T}(\widehat{\lambda}_j^{N_4}), \mathcal{V}(\boldsymbol{\mu}^{N_4})) \leq \sin \phi_{\max}(\mathcal{T}(\widehat{\lambda}_k^{N_4}), \mathcal{V}(\boldsymbol{\mu}^{N_4})) \quad \forall j = 1, \dots, r.$$

We can bound the subspace angle on the right by applying Theorem 4.2, noting that since $N_4 > N_3$ there are at least four μ_\star^ℓ in a ϵ ball around $\widehat{\mu}$ and consequently $\mu_\star^{N_4}$ is at most 2ϵ away from at least three of these

$$(A.43) \quad \sin \phi_{\max}(\mathcal{T}(\widehat{\lambda}_k^{N_4}), \mathcal{V}(\boldsymbol{\mu}^{N_4})) = \|Q(\widehat{\lambda}_k^{N_4})[I - P(\boldsymbol{\mu}^\ell)]\|_{\mathcal{H}_2} \leq 2C'_k \epsilon.$$

Then if we consider the remaining terms of (A.40), inserting the identity $Q(\widehat{\lambda}_j^{N_4}) + [I - Q(\widehat{\lambda}_j^{N_4})]$ and applying the triangle inequality:

$$(A.44) \quad \|Q(\widehat{\lambda}_j)[I - P(\boldsymbol{\mu}^{N_4})]\|_{\mathcal{H}_2} \leq \|Q(\widehat{\lambda}_j)Q(\widehat{\lambda}_j^{N_4})[I - P(\boldsymbol{\mu}^{N_4})]\|_{\mathcal{H}_2} \\ + \|Q(\widehat{\lambda}_j)[I - Q(\widehat{\lambda}_j^{N_4})][I - P(\boldsymbol{\mu}^{N_4})]\|_{\mathcal{H}_2}.$$

Pulling the first projector out of the first term, the last projector out of the second term and then noting that both have norm one,

$$(A.45) \quad \|Q(\widehat{\lambda}_j)[I - P(\boldsymbol{\mu}^{N_4})]\|_{\mathcal{H}_2} \leq \|Q(\widehat{\lambda}_j^{N_4})[I - P(\boldsymbol{\mu}^{N_4})]\|_{\mathcal{H}_2} + \|Q(\widehat{\lambda}_j)[I - Q(\widehat{\lambda}_j^{N_4})]\|_{\mathcal{H}_2}.$$

Then by replacing these norms with their equivalent subspace angle definitions,

$$(A.46) \quad \|Q(\widehat{\lambda}_j)[I - P(\boldsymbol{\mu}^{N_4})]\|_{\mathcal{H}_2} \leq \sin \phi_{\max}(\mathcal{T}(\widehat{\lambda}_j^{N_4}), \mathcal{V}(\boldsymbol{\mu}^{N_4})) + \sin \phi_{\max}(\mathcal{T}(\widehat{\lambda}_j^{N_4}), \mathcal{T}(\widehat{\lambda}_j))$$

we can employ (A.42) to bound the first term and invoking Lemma A.1 we can bound the second leaving

$$(A.47) \quad \|Q(\widehat{\lambda}_j)[I - P(\boldsymbol{\mu}^{N_4})]\|_{\mathcal{H}_2} \leq 2C'_k\epsilon + C_j\epsilon.$$

Hence combining these terms we obtain the bound

$$(A.48) \quad \|Q(\widehat{\lambda})[I - P(\boldsymbol{\mu}^{N_4})]\|_{\mathcal{H}_2} \leq 2C'_k\epsilon + \sum_{\substack{j=1 \\ j \neq k}}^r [2C'_k\epsilon + C_j\epsilon].$$

As increasing the dimension of the orthogonal projector $P(\boldsymbol{\mu}^{N_4})$ cannot increase this bound, this result holds for all $\ell \geq N_4$.

Finally, we bound the third term in (A.29). As $\widehat{H}_r^\ell \rightarrow \widehat{H}_r$, there must be some N_5 such that $\|\widehat{H}_r - \widehat{H}_r^\ell\|_{\mathcal{H}_2} < \epsilon$. Then for $\widehat{N} = \max(N_2, N_3, N_5)$ we can combine the bounds from (A.39) and (A.48) yielding the bound

$$(A.49) \quad \|Q(\widehat{\lambda})[H - \widehat{H}_r]\|_{\mathcal{H}_2} \leq \epsilon \|H - \widehat{H}_r^\ell\|_{\mathcal{H}_2} [2rC'_k - C_j + \sum_{j=1}^r 2C_j] + \epsilon \quad \forall \ell \geq \widehat{N}.$$

As $\|H - \widehat{H}_r^\ell\|_{\mathcal{H}_2}$ is bounded and ϵ was arbitrary, we conclude $\|Q(\widehat{\lambda})[H - \widehat{H}_r]\|_{\mathcal{H}_2} = 0$. \square

Acknowledgements. The authors would like to thank Christopher Beattie, Zlatko Drmač, Mark Embree, Serkan Gugercin, Christian Himpe, Petar Mlinarić, Neeraj Sarna, and the anonymous reviewers for their feedback during the preparation of this manuscript. The first author would like to also thank the Einstein Foundation Berlin and Paul Constantine for their support.

REFERENCES

- [1] K. AHUJA, E. DE STURLER, S. GUGERCIN, AND E. R. CHANG, *Recycling BiCG with an application to model reduction*, SIAM J. Sci. Comput., 34 (2012), pp. A1925–A1949, <https://doi.org/10.1137/100801500>.

- [2] B. D. O. ANDERSON AND A. C. ANTOULAS, *Rational interpolation and state-variable realizations*, Linear Algebra Appl., 138 (1990), pp. 479–509, [https://doi.org/10.1016/0024-3795\(90\)90140-8](https://doi.org/10.1016/0024-3795(90)90140-8).
- [3] A. C. ANTOULAS, *Approximation of Large-Scale Dynamical Systems*, SIAM, Philadelphia, PA, 2005, <https://doi.org/10.1137/1.9780898718713>.
- [4] N. ARONSAJN, *Theory of reproducing kernels*, Trans. Amer. Math. Soc., 68 (1950), pp. 337–404, <https://doi.org/10.1090/S0002-9947-1950-0051437-7>.
- [5] C. BEATTIE AND S. GUGERCIN, *Interpolatory projection methods for structure-preserving model reduction*, Systems Control Lett., 58 (2009), pp. 225–232, <https://doi.org/10.1016/j.sysconle.2008.10.016>.
- [6] C. BEATTIE AND S. GUGERCIN, *Realization-independent \mathcal{H}_2 -approximation*, in Decision and Control (CDC), 2012 IEEE 51st Annual Conference on, IEEE, 2012, pp. 4953–4958, <https://doi.org/10.1109/CDC.2012.6426344>.
- [7] C. BEATTIE AND S. GUGERCIN, *Model reduction by rational interpolation*, in Model Reduction and Approximation, P. Benner, A. Cohen, M. Ohlberger, and K. Wilcox, eds., SIAM, 2017, ch. 7, pp. 297–334, <https://doi.org/10.1137/1.9781611974829.ch7>.
- [8] C. BEATTIE, S. GUGERCIN, AND S. WYATT, *Inexact solves in interpolatory model reduction*, Linear Algebra Appl., 436 (2012), pp. 2916–2943, <https://doi.org/10.1016/j.laa.2011.07.015>.
- [9] C. A. BEATTIE AND S. GUGERCIN, *Inexact solves in Krylov-based model reduction*, in Decision and Control, 2006 45th IEEE Conference on, IEEE, 2006, pp. 3405–3411, <https://doi.org/10.1109/CDC.2006.376798>.
- [10] C. A. BEATTIE AND S. GUGERCIN, *A trust region method for optimal \mathcal{H}_2 model reduction*, in Joint 48th IEEE Conference on Decision and Control and 28th Chinese Control Conference, 2009, pp. 5370–5375, <https://doi.org/10.1109/CDC.2009.5400605>.
- [11] P. BENNER, A. COHEN, M. OHLBERGER, AND K. WILCOX, eds., *Model Reduction and Approximation: Theory and Algorithms*, SIAM, Philadelphia, PA, 2017, <https://doi.org/10.1137/1.9781611974829>.
- [12] Å. BJÖRCK AND G. H. GOLUB, *Numerical methods for computing angles between linear subspaces*, Math. Comput., 27 (1973), pp. 579–594, <https://doi.org/10.1090/S0025-5718-1973-0348991-3>.
- [13] T. BOROS, T. KAILATH, AND V. OLSHEVSKY, *Pivoting and backwards stability of fast algorithms for solving Cauchy linear equations*, Linear Algebra Appl., 343–344 (2002), pp. 63–99, [https://doi.org/10.1016/S0024-3795\(01\)00519-5](https://doi.org/10.1016/S0024-3795(01)00519-5).
- [14] J. P. BOYD, *Exponentially convergent Fourier-Chebyshev quadrature schemes on bounded and infinite intervals*, J. Sci. Comput., 2 (1987), pp. 99–109, <https://doi.org/10.1007/BF01061480>.
- [15] M. A. BRANCH, T. F. COLEMAN, AND Y. LI, *A subspace, interior, and conjugate gradient method for large-scale bound-constrained minimization problems*, SIAM J. Sci. Comput., 21 (1999), pp. 1–23, <https://doi.org/10.1137/S1064827595289108>.
- [16] T. BUI-THANH, K. WILLCOX, AND O. GHATTAS, *Model reduction for large-scale systems with high-dimensional parametric input space*, SIAM J. Sci. Comput., 30 (2008), pp. 3270–3288, <https://doi.org/10.1137/070694855>.
- [17] A. CASTAGNOTTO, H. K. PANZER, AND B. LOHMANN, *Fast \mathcal{H}_2 -optimal model order reduction exploiting the local nature of Krylov-subspace methods*, in Control Conference (ECC), 2016 European, IEEE, 2016, pp. 1958–1969, <https://doi.org/10.1109/ECC.2016.7810578>.
- [18] Y. CHAHLAOUI AND P. V. DOOREN, *A collection of benchmark examples for model reduction of linear time invariant dynamical systems*, tech. report, SLICOT, Feb. 2002, <http://slicot.org/objects/software/reports/SLWN2002-2.ps.gz>. Working Note 2002-2.
- [19] E. DE STURLER, S. GUGERCIN, M. E. KILMER, S. CHATURANTABUT, C. BEATTIE, AND M. O’CONNELL, *Nonlinear parametric inversion using interpolatory model reduction*, SIAM J. Sci. Comput., 37 (2015), pp. B495–B517, <https://doi.org/10.1137/130946320>.
- [20] J. DEMMEL, *Accurate singular value decompositions of structured matrices*, SIAM J. Matrix Anal. Appl., 21 (2000), pp. 562–580, <https://doi.org/10.1137/S0895479897328716>.
- [21] P. V. DOOREN, K. A. GALLIVAN, AND P.-A. ABSIL, *\mathcal{H}_2 -optimal model reduction of MIMO systems*, Appl. Math. Lett., 21 (2008), pp. 1267–1273, <https://doi.org/10.1016/j.aml.2007.09.015>.
- [22] P. V. DOOREN, K. A. GALLIVAN, AND P.-A. ABSIL, *\mathcal{H}_2 -optimal model reduction with higher-order poles*, SIAM J. Matrix Anal. Appl., 31 (2010), pp. 2738–2753, <https://doi.org/10.1137/080731591>.
- [23] Z. DRMAČ, S. GUGERCIN, AND C. BEATTIE, *Quadrature-based vector fitting for discretized \mathcal{H}_2 approximation*, SIAM J. Sci. Comput., 37 (2015), pp. A625–A652, <https://doi.org/10.1137/>

- 140961511.
- [24] G. FLAGG, C. BEATTIE, AND S. GUGERCIN, *Convergence of the iterative rational krylov algorithm*, *Systems Control Lett.*, 61 (2012), pp. 688–691.
 - [25] W. GAWRONSKI, *Advanced Structural Dynamics and Active Control of Structures*, Springer Science & Business Media, 2004.
 - [26] G. H. GOLUB AND V. PEREYRA, *The differentiation of pseudo-inverses and nonlinear least squares problems whose variables separate*, *SIAM J. Numer. Anal.*, 10 (1973), pp. 413–432, <https://doi.org/10.1137/0710036>.
 - [27] E. J. GRIMME, *Krylov Projection Methods for Model Reduction*, PhD thesis, University of Illinois at Urbana-Champaign, 1997.
 - [28] S. GUGERCIN, A. C. ANTOULAS, AND C. BEATTIE, \mathcal{H}_2 model reduction for large-scale linear dynamical systems, *SIAM J. Matrix Anal. Appl.*, 30 (2008), pp. 609–638, <https://doi.org/10.1137/060666123>.
 - [29] B. GUSTAVSEN AND A. SEMLYEN, *Rational approximation of frequency domain responses by vector fitting*, *IEEE T. Power Deliver.*, 14 (1999), pp. 1052–1061, <https://doi.org/10.1109/61.772353>.
 - [30] J. M. HOKANSON, *Projected nonlinear least squares for exponential fitting*, *SIAM J. Sci. Comput.*, 39 (2017), pp. A3107–A3128, <https://doi.org/10.1137/16M1084067>.
 - [31] J. M. HOKANSON AND C. C. MAGRUDER, *Least squares rational approximation*, 2018, <https://arxiv.org/abs/1811.12590>.
 - [32] E. JONES, T. OLIPHANT, P. PETERSON, ET AL., *SciPy: Open source scientific tools for Python*, 2001–, <http://www.scipy.org/>. [Online; accessed 1 Oct 2018].
 - [33] T. KATO, *Perturbation theory for linear operators*, Springer-Verlag, Berlin, 1995. Reprint of the 1980 edition.
 - [34] R. B. LEHOUCQ, D. C. SORENSEN, AND C. YANG, *ARPACK User’s Guide: Solution of Large-Scale Eigenvalue Problems with Implicitly Restarted Arnoldi Methods*, SIAM, Philadelphia, 1998, <https://doi.org/10.1137/1.9780898719628>.
 - [35] L. MEIER AND D. LUENBERGER, *Approximation of linear constant systems*, *IEEE T. Automat. Contr.*, 12 (1967), pp. 585–588, <https://doi.org/10.1109/TAC.1967.1098680>.
 - [36] L. MEIER III, *Approximation of Linear Constant Systems by Linear Constant Systems of Lower Order*, PhD thesis, Stanford University, 1965.
 - [37] Y. NAKATSUKASA, O. SÈTE, AND L. N. TREFETHEN, *The AAA algorithm for rational approximation*, *SIAM J. Sci. Comput.*, 40 (2018), pp. A1494–A1522, <https://doi.org/10.1137/16M1106122>.
 - [38] M. O’CONNELL, M. E. KILMER, E. DE STURLER, AND S. GUGERCIN, *Computing reduced order models via inner-outer Krylov recycling in diffuse optical tomography*, *SIAM J. Sci. Comput.*, 39 (2017), pp. B272–B297, <https://doi.org/10.1137/16M1062880>.
 - [39] C. K. SANATHANAN AND J. KOERNER, *Transfer function synthesis as a ratio of two complex polynomials*, *IEEE T. Automat. Contr.*, 8 (1963), pp. 56–58, <https://doi.org/10.1109/TAC.1963.1105517>.
 - [40] P. J. SCHREIER AND L. L. SCHARF, *Statistical Signal Processing of Complex-Valued Data: Theory of Improper and Noncircular Signals*, Cambridge University Press, Cambridge, 2010.
 - [41] G. SHI, *On the nonconvergence of the vector fitting algorithm*, *IEEE T. Circuits-II*, 63 (2016), pp. 718–722.
 - [42] T. STYKEL AND A. VASILYEV, *A two-step model reduction approach for mechanical systems with moving loads*, *J. Comput. Appl. Math.*, 297 (2016), pp. 85–97, <https://doi.org/10.1016/j.cam.2015.11.014>.
 - [43] T. WOLF, H. K. F. PANZER, AND B. LOHMANN, \mathcal{H}_2 pseudo-optimality in model order reduction by Krylov subspace methods, in *2013 European Control Conference*, 2013, pp. 3427–3432, <https://doi.org/10.23919/ECC.2013.6669585>.
 - [44] A. YOUSUFF, D. A. WAGIE, AND R. E. SKELTON, *Linear system approximation via covariance equivalent realizations*, *J. Math. Anal. Appl.*, 106 (1985), pp. 91–115, [https://doi.org/10.1016/0022-247X\(85\)90133-7](https://doi.org/10.1016/0022-247X(85)90133-7).